**Universidade do Minho**
Escola de Engenharia

Ana Luísa Afonso de Carvalho

# Validation of siRNAs against MAP2K1/MEK1 towards colon cancer therapy

julho de 2018

Validation of siRNAs against MAP2K1/MEK1 towards colon cancer therapy
Ana Luísa Afonso de Carvalho
UMinho | 2018

**Universidade do Minho**
Escola de Engenharia

Ana Luísa Afonso de Carvalho

# Validation of siRNAs against MAP2K1/MEK1 towards colon cancer therapy

Dissertação de Mestrado
Mestrado Integrado em Engenharia de Biomédica

Trabalho realizado sob orientação da
**Professora Doutora Lígia Raquel Marona Rodrigues**

julho de 2018

DECLARAÇÃO

Nome: Ana Luísa Afonso de Carvalho

Endereço eletrónico: a73324@alunos.uminho.pt Telefone: 915354784

Bilhete de Identidade/Cartão do Cidadão: 14916353

Título da dissertação: Validation of siRNAs against MAP2K1/MEK1 towards colon cancer therapy

Orientadora:

Professora Doutora Lígia Raquel Marona Rodrigues

Ano de conclusão: 2018

Mestrado Integrado em Engenharia de Biomédica

DE ACORDO COM A LEGISLAÇÃO EM VIGOR, NÃO É PERMITIDA A REPRODUÇÃO DE QUALQUER PARTE DESTA DISSERTAÇÃO.

Universidade do Minho, _____/_____/_____

Assinatura:

# ACKNOWLEDGEMENTS

A realização deste trabalho de investigação foi apenas possível devido ao estímulo, empenho e auxílio de diversas pessoas a quem gostava de dar uma palavra de agradecimento.

Agradeço à Professora Lígia Rodrigues por todas as sugestões e orientações que me foi dando ao longo de todo o projeto e por estar sempre disponível a ajudar.

Á Débora Ferreira por todo o auxílio, pela paciência e facilidade com que me transmitiu conhecimentos e esclarecimentos e, acima de tudo, pela disponibilidade e boa disposição em todas as horas.

Ás minhas colegas do Laboratório de Bioprocessos e Bioprodutos Sustentáveis, Cátia Silva e Rute Tavares agradeço pelos conselhos, pelo auxílio no projeto, pelo bom ambiente de trabalho que me proporcionaram e sobretudo pela amizade.

Ao Mário pela paciência, por todo o carinho, presença e apoio incansável ao longo deste percurso o meu mais sincero agradecimento. Agradeço ainda às minhas amigas, Mariana Ferreira, Mariana Silva, Ana Rita Martins e Ana Teresa Araújo que sempre me apoiaram em todos os projetos e com quem ultrapassei obstáculos.

Aos meus pais, irmã e à minha família mais próxima que, estando ou não presentes no meu dia a dia, me incentivaram em todos os momentos, quero agradecer pelo esforço, por contribuírem para que atingisse os meus objetivos e sobretudo por todo o afeto.

# ABSTRACT

Cancer can be considered a public health problem due to their high incidence and mortality rates. Specifically, colon cancer is the fourth most common and the second deadliest worldwide. The major part of colon cancers occurs due to a family predisposition although some of them can also be related with environmental factors such as smoke, alcohol consumption and a diet rich on fat. Colon cancer therapies depend on the disease stage and rely mostly on surgery and chemotherapy, either adjuvant or neoadjuvant. However, chemotherapy has a few shortcomings as immunosuppression and lack of specificity for instance. Therefore, more specific therapies are need. The use of siRNAs is one of these possibilities since they are able to target specific genes that are often overexpressed on cancer cells. The MAPK pathway plays an important role on cell proliferation, differentiation and apoptosis in mammalian cells. The aberrant activation of this pathway and of *MEK1*, specifically, is often observed in cancer. So, the goal of this work was the validation of a siRNA targeting *MEK1* gene towards colon cancer therapy. *MEK1* gene is overexpressed in several colorectal cancer cell lines. Our results showed that the colon cancer cell line with higher expression of *MEK1* gene is RKO, so this was the cell line that we used further in the study. RKO cells were transfected with an optimized siRNA concentration of 30 nM and the *MEK1* gene knockdown effects on cell cycle and cell proliferation were studied. Moreover, the siRNA transfection efficiency was also evaluated through Western Blot and qRT-PCR. Additionally, it has been reported that *MEK1* gene knockdown often leads to a cell cycle arrest on GO-G1 phase. Our results corroborate these reports as a cell cycle arrest on GO-G1 phase was observed, indicating a probable decrease on cell proliferation since the cells do not progress to the S phase. Therefore, SRB and MTS proliferation assays were performed. Although the SRB results were inconclusive, the MTS results confirmed a significant decrease of cell viability on the cells transfected. This could mean that, besides the number of cells remained constant, they may be non-metabolically active. Furthermore, the MEK1_siRNA transfection was considered efficient since it was able to knockdown *MEK1* about 52.5% at protein level and about 61.6% at the mRNA level. Additionally, the *MEK1* knockdown effect on *ERK1* gene, which is located downstream *MEK1* gene, was also assessed. Results showed a 52.1% knockdown on the *ERK1* gene, thus confirming its effect on cell proliferation. Overall, the results herein gathered are in good agreement with previous reports, thus highlighting the siRNA potential for cancer therapy.



**Keywords**: siRNA, MAPK, MEK1, gene silencing, colon cancer

# SUMÁRIO

O cancro pode ser considerado um problema de saúde pública tendo em conta as suas taxas de incidência e mortalidade. O cancro do cólon é o quarto cancro mais comum e o segundo mais mortal em todo o mundo. A maioria ocorre devido a uma predisposição familiar, embora alguns estejam relacionados com fatores ambientais tais como o consumo de tabaco e/ou álcool e uma dieta rica em gordura. As terapias usadas dependem do seu estágio e baseiam-se principalmente em cirurgia e quimioterapia. No entanto, a quimioterapia tem desvantagens tais como a imunodepressão ou a falta de especificidade, entre outras. Assim, são necessárias terapias mais especificas. O uso de siRNAs é uma das possibilidades pois estes são capazes de afetar genes específicos que estão muitas vezes sobre-expressos em células cancerígenas. A via de sinalização MAPK tem um papel importante na proliferação, diferenciação e apoptose de células animais. A sua ativação aberrante e em particular do gene *MEK1* é muito comum. Assim, o objetivo deste trabalho foi a validação de um siRNA, tendo como alvo o gene *MEK1*, como potencial terapia do cancro do cólon. O *MEK1* é um gene sobre-expresso em várias linhas celulares colorretais. Os resultados demonstraram que a linha celular do cólon com maior expressão de *MEK1* é a RKO, tendo, portanto, o restante estudo sido baseado nesta linha celular. As células RKO foram transfectadas com uma concentração otimizada de 30 nM de siRNA e o efeito do silenciamento do *MEK1* no ciclo celular e na proliferação celular foi estudado. Adicionalmente, a eficiência da transfecção também foi avaliada através de *Western Blot* e qRT-PCR. A paragem do ciclo celular na fase G0-G1 como resultado do silenciamento do gene *MEK1* tem sido reportado. Os nossos resultados corroboram esses relatos tendo-se observado uma paragem do ciclo em G0-G1, o que indica uma provável diminuição da proliferação celular. Assim, foram realizados os testes SRB e MTS. Os resultados de SRB foram inconclusivos, mas os resultados de MTS demonstraram uma significativa diminuição da viabilidade celular das células transfectadas. Isto pode significar que, apesar do número de células ter sido constante, as mesmas podem não estar metabolicamente ativas. Para além disso, a transfecção de MEK1_siRNA foi considerada eficiente uma vez que silenciou o gene *MEK1* em cerca de 52,5% a nível proteico e em cerca de 61,6% a nível do mRNA. Por último, também se avaliou o efeito do silenciamento de *MEK1* no gene *ERK1,* que se encontra localizado abaixo do gene *MEK1* na via de sinalização, confirmando, portanto, o seu efeito na proliferação celular. Genericamente, os resultados gerados estão em concordância com estudos anteriores, reforçando o potencial do siRNA para efeitos terapêuticos.

**Palavras-chave:** siRNA, MAPK, MEK1, silenciamento de genes, cancro do cólon

# TABLE OF CONTENTS

# TABLE OF CONTENTS (CONT.)

# LIST OF FIGURES

# LIST OF FIGURES (CONT.)

# LIST OF FIGURES (CONT.)

# LIST OF TABLES

# LIST OF ABBREVIATIONS

**AGO2:** Argonaute 2

**APC:** Adenomatous polyposis coli

**BCA:** Bicinchoninic Acid

**BLAST:** Basic Local Alignment Search Tool

**BSA:** Bovine Serum Albumin

**CIMP:** CpG island methylator phenotype

**CIN:** Chromosomal instability

**CPP:** Cell penetrating peptides

**DAPI:** 4',6-diamidino-2-phenylindole

**DMEM:** Dulbecco Modified Eagle Medium

**DNA:** Deoxyribonucleic acid

**dsRNA:** Double stranded Ribonucleic acid

**EDTA:** Ethylenediaminetetraacetic acid

**EGFR:** Epidermal Growth Factor Receptor

**ERK1:** Extracellular signal-regulated kinase

**FAP:** Familial Adenomatous Polyps

**FBS:** Fetal Bovine Serum

**GADPH:** Glyceraldehydes-3-phosphate dehydrogenase

**GTP:** Guanosine triphosphate

**HNPCC:** Hereditary Non-Polyposis Colorectal Cancer

**JNK or SAPK:** c-Jun N-terminal or stress activated kinases

**LOH:** Loss of heterozygosity

**MAPK:** Mitogen activated protein kinase

**MEK1:** Mitogen activated protein kinase kinase

**MMR:** Mismatch repair

**mRNA:** Messenger RNA

**MSI:** Microsatellite instability

**MTS:** 3-(4,5-dimethylthiazol-2-yl)-5(3-carboxymethonyphenol)-2-(4-sulfophenyl)-2H-tetrazolium

**NC_siRNA:** Negative control small interfering ribonucleic acid

**NRT:** No reverse transcriptase

**NTC:** No template control

**ORF:** Opening reading frame

**PBS:** Phosphate Buffered Saline

**PFA:** Paraformaldehyde

**PUFAs:** Polyunsaturated fatty acids

**qRT-PCR:** Reverse transcription polymerase chain reaction

**RES:** Reticuloendothelial system

**RISC:** Ribonucleic acid induced silencing complex

**RNA:** Ribonucleic acid

**RNAi:** Ribonucleic acid interference

**RNase A:** Ribonuclease A

**RPMI:** Roswell Park Memorial Institute

**RTKs:** Tyrosine kinase receptors

**SDS:** Sodium Dodecyl Sulfate

**SDS – PAGE:** Sodium Dodecyl Sulfate – PolyAcrylamide Gel Electrophoresis

**siRNA:** small interfering ribonucleic acid

**SOS:** Son of sevenless

**SRB:** Sulforhodamine B

**TBS T:** Tris-buffered saline with Tween 20

**TEMED:** Tetramethylethylenediamine

**TGS:** Tris - Glycine - SDS buffer

## List of Abbreviations (Cont.)

**VEGF:** Vascular Endothelial Growth Factor

**WAVE-2:** Wiskott-Aldrich syndrome protein family member 2

**WHO:** World Health Organization

# 1. INTRODUCTION

## 1.1 Colon cancer

Cancer is one of the most incident and mortal pathologies in the World (Ferlay et al., 2015). Only in 2017, in the United States, about 95.5 thousand people (both man and women) were diagnosed with this disease and 50.3 thousand people died (Siegel, Miller, & Jemal, 2017). Globally, colon cancer is the fourth most common and the second deadliest (Fredericks, Dealtry, & Roux, 2015). According to the WHO (World Health Organization) estimates for 2015, colorectal cancer appears as the third most malignant cancer in Europe, being the lung and the liver cancers the leading cause of deaths ("WHO | Estimates for 2000–2015," 2017).

Considering the demographical morbidity and mortality of colon cancer it is notable that this disease is more common in high income countries rather than low income countries ("WHO | Estimates for 2000–2015," 2017). This difference can possibly be explained by the different dietary habits (Celalettin, 2004). In fact, one of the main environmental factors that can increase colon cancer development risk is overweight. The consumption of red and processed meat, as well as fast food, which is more common in Western countries, may also contribute to this problem. On the other hand, studies show that diets with high incomes of fish oils like omega-3 PUFAs (polyunsaturated fatty acids) (Pietrzyk, 2017), calcium (Han et al., 2015), vitamin D (Barbáchano, Larriba, Ferrer-Mayorga, González-Sancho, & Muñoz, 2018) and even probiotics (Seidel, Azcárate-Peril, Chapkin, & Turner, 2017), for example, can protect the organism against colon cancer. A diet rich in fibers, fruit and vegetables rather than in fat can be a preventive measure, as well as a less sedentary lifestyle (Celalettin, 2004; Pan, Yu, & Wang, 2018). Besides the diet factor, there are other environmental precursors of this disease such as smoking, alcohol consumption and aging. Colon cancer is also associated to a hereditary predisposition, mostly among first degree relatives (Druliner et al., 2018).

## 1.2 Colon cancer carcinogenesis

As previously mentioned, environmental, as well as genetic factors play an important role in colon cancer development and progression. In this multi-step process, colon mucosa will suffer genomic modifications over the years which will lead eventually to the polyp evolution to a carcinoma. However, 80-85% colon cancers have sporadic appearance and only 15-20% are hereditary ones, such as FAP (Familial Adenomatous Polyps) or HNPCC (Hereditary Non-Polyposis Colorectal Cancer) (Fredericks et

al., 2015; Zuckerman & Davis, 2015). Usually, the first ones occur in higher risk groups such as elder people for example.

Colorectal cancers are normally based in a combination of three different mechanisms (Figure 1): CIN (chromosomal instability); CIMP (CpG island methylator phenotype) and MSI (microsatellite instability) (Laporte, Leguisamo, Kalil, & Saffi, 2018; Tariq & Ghias, 2016).

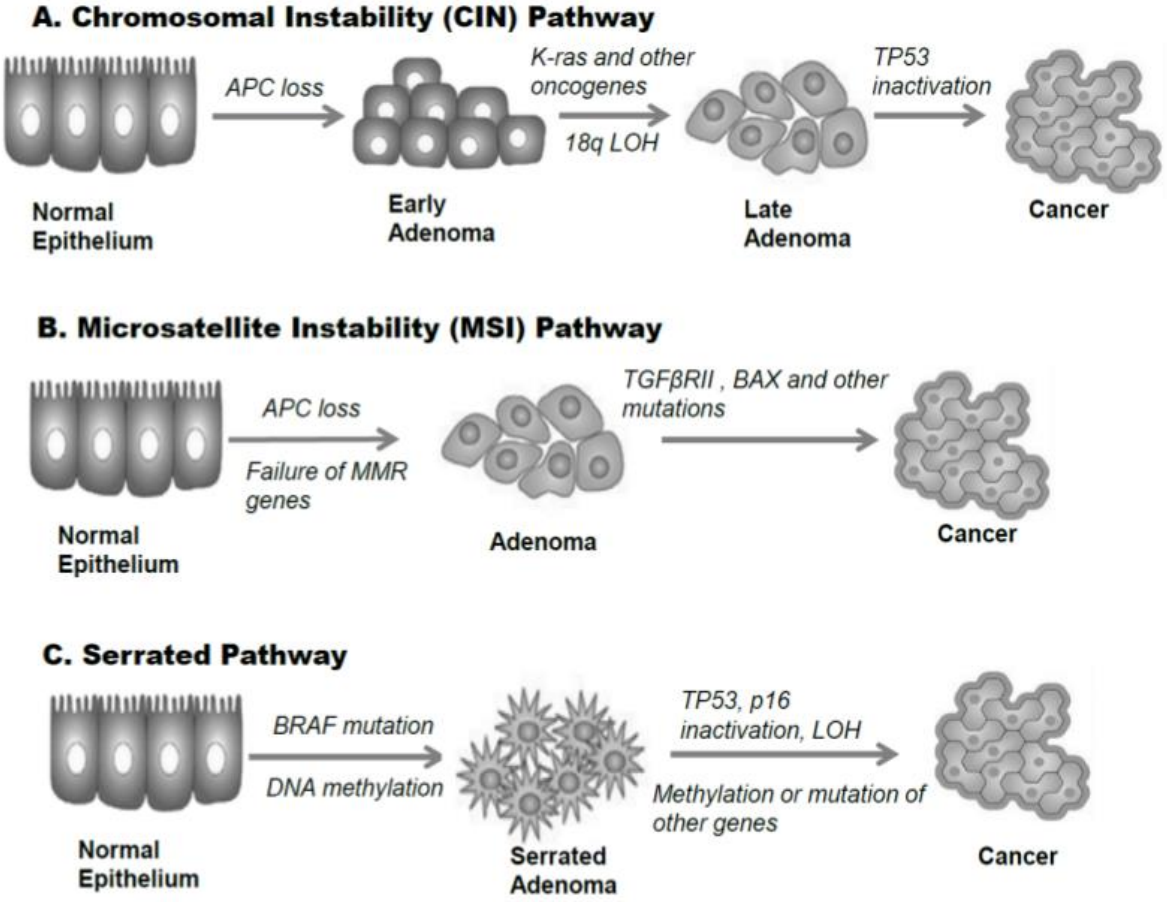


**Figure 1** - Sequential genetic and epigenetic changes in the different mechanisms that lead to colorectal cancer pathogenesis (Taken from (Mundade, Imperiale, Prabhu, Loehrer, & Lu, 2014)).

Usually, about 85% of sporadic colon cancers occur due to CIN. The CIN pathway follows the adenoma-carcinoma sequence model (Mundade, Imperiale, Prabhu, Loehrer, & Lu, 2014), proposed in 1990 by Vogelstein and Fearon, and is characterized for its aneuploidy, LOH (loss of heterozygosity), multiple chromosomal rearrangements and accumulation of mutation on oncogenes such as K-RAS or even on tumor suppressor genes like APC (adenomatous polyposis coli) or p53. *APC* is inactivated in a great number of colon cancers and has an important role preventing the accumulation of molecules usually associated with cancer development (Hardy, 2000; Mundade et al., 2014). The mutations that

this gene may suffer include insertions, deletions or nonsense mutations that will ultimately lead to *APC* loss of function (Fredericks et al., 2015; Tariq & Ghias, 2016).

CIMP, also known as Serrated Pathway, is characterized by epigenetic events such as DNA (deoxyribonucleic acid) hypomethylation and localized promoter hypermethylation, as well as for the presence of mutations in BRAF oncogene (Mundade et al., 2014).

Regarding MSI, only 15% of sporadic colon cancers are caused by MSI. MSI occurs usually in oncogenes and in tumor suppressor gene due to mutations in the DNA MMR (mismatch repair) genes that should amend DNA replication errors (Laporte et al., 2018) or because of aberrant methylation of CpG (Mundade et al., 2014).

Near 1% of colon cancers are due to FAP, a family disease associated to a mutation in the *APC* gene. People suffering from this illness, around late youth, develop a lot of adenomas that increase their predisposition for colorectal cancer (Fredericks et al., 2015; Kennelly, Gryfe, & Winter, 2017). Moreover, about 5% of all colon cancers are a consequence of HNPCC. HNPCC, also known as Lynch syndrome, is an inherited autosomal dominant disease with an error on mismatch repair genes leading to MSI (Kennelly et al., 2017).

### 1.2.1 MAPK pathway

One of the most important colon cancer precursors are the mutations in *KRAS* and *BRAF* genes. Mutations on these genes lead to the constitutive activation, i.e. at a constant level, of the MAPK (Mitogen Activated Protein Kinase) pathway (Fang & Richardson, 2005). This pathway plays an important role on cell proliferation, differentiation, transformation and apoptosis in mammalian cells (W. Zhang & Liu, 2002) and is often activated in colon cancers (Oh et al., 2016). MAPK pathway can also be activated by extracellular signals, such as growth factors, that are recognized by the membrane receptors and trigger signal transduction cascades (Fang & Richardson, 2005). Generally, MAPK can be divided in three major serine-threonine kinases families, namely the ERK-MAPK (extracellular signal regulated kinases), the JNK or SAPK (c-Jun N-terminal or stress activated kinases) and the MAPK14 or p38 kinase (Fang & Richardson, 2005; Urosevic, Nebreda, & Gomis, 2014).

The ERK-MAPK pathway (Figure 2), also known as Raf-MEK-ERK, is the most studied effector pathway downstream Ras and the best caracterized of all MAPK families (Fang & Richardson, 2005; W. Zhang & Liu, 2002).

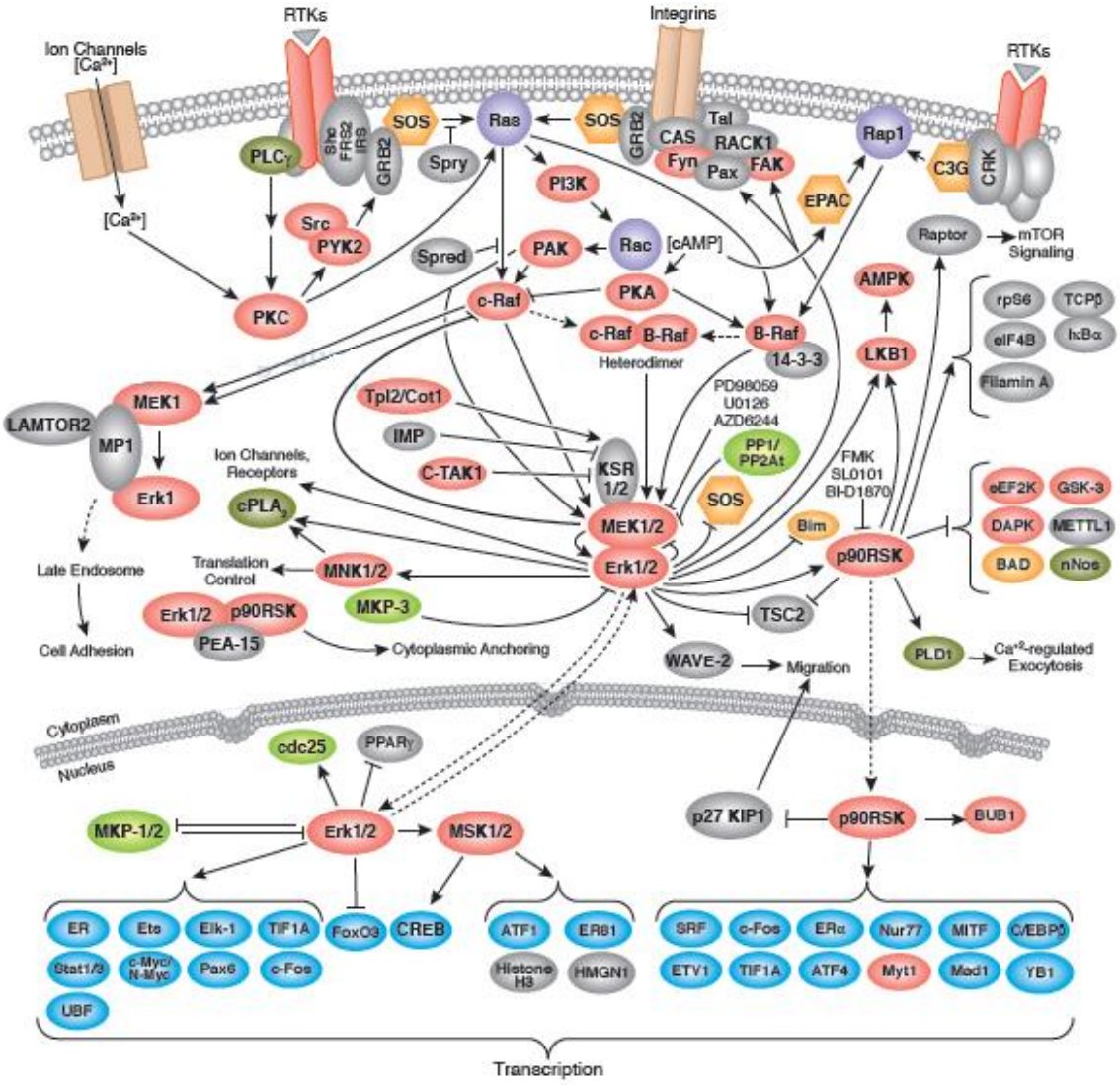


**Figure 2** - The ERK-MAPK pathway in mammalian cells. (Taken from Cell Signaling website: https://www.cellsignal.com/contents/science-cst-pathways-mapk-signaling/mapk-erk-in-growth-and-differentiation-signaling-interactive-pathway/pathways-mapk-erk, accessed on March 23rd of 2018).

RTKs (Transmembrane tyrosine kinase receptors) proteins respond to external stimuli, such as growth factors, hormones and chemokines. This interaction will prevent adaptor cytoplasmic proteins to link to them and will trigger downstream chain of processes and reactions (De Luca, Maiello, D'Alessio, Pergameno, & Normanno, 2012; W. Zhang & Liu, 2002). Basically, this pathway is composed by a G protein (RAS protein) and three protein kinases, namely RAF, MEK and ERK (W. Zhang & Liu, 2002).

As previously mentioned, the adaptor proteins cannot connect with RTKs and therefore, will attract effectors like guanine-nucleotide exchange factor SOS (son of sevenless) to the plasmatic membrane that will activate the RAS protein. When this protein is active, i.e., when it is connected to GTP (guanosine

triphosphate), it is able to activate the effector protein kinase RAF. Consequently, their isoforms will phosphorylate the protein kinase MEK. This protein kinase has dual-specificity kinases that will recognize and activate the next enzyme in the chain, ERK. ERK also has double specificity to tyrosine and to serine-threonine amino acids residues (De Luca et al., 2012; W. Zhang & Liu, 2002). Only when both subunits are phosphorylated, the ERK behaves as an enzyme and is able to pass to the cell nucleus, where it can phosphorylate and activate transcription factors.

The MEK1 or MAP2K1 (mitogen activated protein kinase kinase) kinase has been proven to be extremely important on the ERK-MAPK pathway due to its unique characteristics. As it can be seen on Figure 2, MEK1 does not have an effect in other gene than ERK, which does not occur with the other MAP kinases, thus highlighting MEK1 selectivity. Moreover, it ability to phosphorylate serine-threonine residues shows the importance of this kinase on the ERK-MAPK pathway. It was also observed in some studies that the MEK1 constitutive activation leads to cellular transformation (Oh et al., 2016; Sebolt-Leopold et al., 1999). Taking into account all these concepts, the *MEK1* will be the target gene in this study.

### 1.2.2 Therapies

Colon cancer treatment is mostly decided upon the stage of the cancer. Stage's classification increases as the cancer depth of invasion develops. Individuals diagnosed with colon cancer on stage 0, I or II are usually submitted just to surgery while people with high recurrence risk cancers on stage II or cancers on stage III are mainly treated with surgery followed by chemotherapy (adjuvant therapy) (Veenstra & Krauss, 2018; Wolpin & Mayer, 2008).

Chemotherapeutic drugs used on colon cancer adjuvant therapy helps to prevent the formation of a new cancer and are mostly based on fluorouracil (Veenstra & Krauss, 2018). This anti-metabolic agent affects the DNA synthesis leading to the inhibition of cancerous cells growth (X.-Q. Zhang, Zhang, Sun, Yuan, & Feng, 2015). Using 5-fluorouracil drug monotherapy or mixing it with oxaliplatin (a cytotoxic drug) and leucovorin (drug modulator) leads to the increase of colon cancer patients survival rates (Veenstra & Krauss, 2018).

People with stage IV colon cancer have to go over neoadjuvant and adjuvant chemotherapy (before and after surgery) when surgery is still a possibility. Neoadjuvant therapy is important because it will help to reduce the cancer size enabling an easier surgery. In some cases, surgery is not an option because at these stage metastasis appear in other organs and, therefore, patients only go over chemotherapy to help minimizing the cancer size and increase patient's lifetime (X.-Q. Zhang et al., 2015).

There are already some therapies, combined with common chemotherapy drugs, that have been used (Veenstra & Krauss, 2018). Angiogenesis inhibitors, for instance, are proven to increase the overall survival of initial metastatic cancers by inhibiting the VEGF (vascular endothelial growth factor) since the tumor vascularity is crucial to its expansion (Bennouna et al., 2013; Veenstra & Krauss, 2018). Another approach is the use of EGFR (epidermal growth factor receptor) inhibitors. However, the phase III trials for this approach have controversial and distinct results as no significant improvements of the outcome could be found when compared with angiogenesis inhibitors and, in some cases, they exhibited worst results than the ones accomplished when using only chemotherapy (Heinemann et al., 2014).

As it is common knowledge, chemotherapy has some side effects such as immunodepression, anorexia (loss of appetite), hair loss or even an increased resistance to chemotherapeutic drugs (McCubrey et al., 2007). Moreover, while stage I colon cancer five-year survival is about 90%, people suffering from stage IV cancer only have an expected five-year survival of 5 to 8% (Wolpin & Mayer, 2008). Therefore, new and more specific therapies are needed.

Other therapies available for colon cancer treatment are radiotherapy, steam cell transplant and immunotherapy (You et al., 2016).

## 1.3 Small interfering RNA (siRNA)

To overcome the chemotherapy barriers, the use of siRNA (small interfering ribonucleic acid) molecules has raised increased interest in the last years because these sequences are highly selective and specific, thus enabling a more effective and less toxic therapy. siRNAs are also easy to synthetize and have a low production cost when compared for instance with antibodies (Jain, Pathak, & Vaidya, 2018).

RNAi (RNA interference) was originally observed in a 1990 study by Napoli and coworkers (Napoli, 1990). The goal was to overexpress an enzyme responsible for plant coloration. However, the gene introduction inhibited the pigment synthesis and it was only later, in a similar experiment that the phenomena was understood. Fire and Melo reported that in nematode *Caenorhabditis elegans* the gene expression could be manipulated using long dsRNAs (double stranded RNAs) (Fire et al., 1998). Despite of silencing gene expression, when it was used in mammalians it was found that long dsRNA are non-specific and may activate the innate immune response by inducing interferon-linked pathways (Rana, 2007). However, it is possible to process these sequences into smaller ones (siRNAs), inducing the sequence-specific of targeted genes (Karim, Tha, Othman, Borhan Uddin, & Chowdhury, 2018).

Besides the mentioned advantages, the siRNA mechanism of action starts in the cytoplasm. This part of the cell is much easier to access than the cell nucleus since the nuclear barrier is a huge obstacle (Karim et al., 2018). Moreover, siRNA is proven to knockdown targets such as oncogenes currently known as "undruggable", like for example RAS (Valentino et al., 2012).

### 1.3.1 Gene silencing

To produce siRNAs, a long dsRNA is cleaved into smaller 21-23 nucleotides siRNA by the RNase III-type enzyme called Dicer (Rana, 2007). The siRNA can be produced synthetically and introduced exogenously in the cells by several transfection methods in order to induce RNAi (Karim et al., 2018; Rana, 2007). siRNA molecules have two strands, that are sense (passenger strand) and antisense (guide strand) with the target mRNA (messenger RNA) (Rana, 2007).

Once the siRNA is in the cell cytoplasm, it will incorporate the RISC (RNA induced silencing complex), forming a RNA-protein complex. The catalytic core of RISC is a protein named AGO2 (Argonaute 2) that is able to separate the siRNA chains and degrades the siRNA sense strand. The antisense strand containing RISC selectively seeks and binds to the target mRNA enabling specific gene silencing (Karim et al., 2018; Rana, 2007). The mentioned complex is responsible for the target mRNA cleavage because cleavage occurs between 10 and 11 nucleotides upstream the sequence 5' end. Afterwards, the activated RISC complex moves on to other mRNA targets until their degradation. This activated RISC complex state only has a therapeutic effect for about 3 to 7 days in highly reproductive cells (such as cancer cells) and for a few weeks in non-dividing cells (Karim et al., 2018; Whitehead, Langer, & Anderson, 2009). The siRNA that do not escape from the endosome will eventually be degraded (Figure 3).

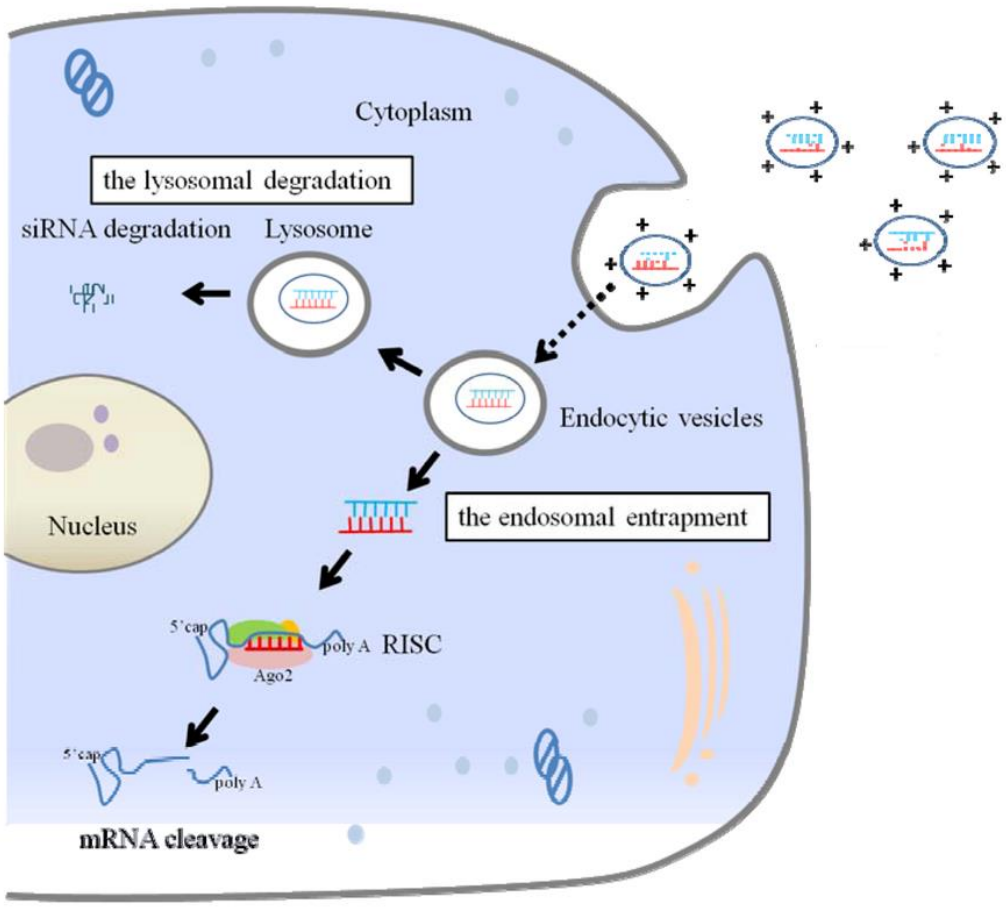


**Figure 3** - siRNA gene silencing mechanism. The siRNA is internalized by the cell through an endocytose process. Once in the cell cytoplasm, the siRNA is release from the endosome and from the nanoparticle. Then, it is connected with the RISC, forming a complex that will separate both siRNA strands. The antisense strand will then bind and cleave the targeted mRNA (Taken from: http://www.mdpi.com/journal/pharmaceuticals/special_issues/rbased-therapeutics, accessed on April 7th of 2018).

Theoretically, it is possible to design any siRNA sequence targeting any potential gene and consequently silencing it. Therefore, this property opens a huge path for a lot of gene-related disease treatment, being expected better results than the ones already accomplished by other therapies such as small molecule inhibition of protein function (Reynolds et al., 2004).

### 1.3.2 siRNA design

The siRNA sequence design is a crucial step for an efficient gene silencing. In the early studies using siRNAs, it was observed that different sequences targeting the same mRNA exhibited opposite outcomes, since only a few led to gene silencing (Buehler, Chen, & Martin, 2012). To design a functional siRNA with optimal gene silencing is necessary to take into account several parameters.

Bioinformatic tools including siDESIGN Center (Dharmacon), siRNA Design (IDT) and Target Finder (Ambion) offer guidelines to select potential siRNA sequences and determine if the siRNA sequences chosen are specific, i.e., if these only match the mRNA targeted.

First, it is necessary to define the gene region that will be targeted for gene knockdown. Nowadays, the choice of these regions is limited to the parts of the gene that can be transcribed, except introns and splice junctions. The most used region is the ORF (opening reading frame) because it has a conserved nature of coding sequences and a low probability of polymorphisms (Birmingham et al., 2007). Moreover, the siRNA duplex should not be longer than 21 nucleotides and shorter than 18 nucleotides and both strands should be fully complementary (Grinev, 2012).

Additionally, it is also crucial to be aware of issues related to thermodynamics or sequence properties. The most important property regarding a functional siRNA is the thermodynamic profile due to the siRNA incorporation into RISC. The antisense strand 5' end should have low stability, which will facilitate the RISC incorporation. Therefore, the siRNA should have higher quantity of A/U nucleotides between the positions 1 to 7 because the single hydrogen bonds formed are weaker than double hydrogen bounds between C/G nucleotides. In summary siRNA sequence should be AA($N_{19}$)TT (Birmingham et al., 2007; Grinev, 2012; Reynolds et al., 2004).

The siRNA central region should be likewise unstable, so, the sequence should have a low quantity of C/G nucleotides (Birmingham et al., 2007; Reynolds et al., 2004). A study performed in 2004 by Reynolds and his co-workers showed that highly functional siRNAs hold a C/G content between 36 and 52% (Reynolds et al., 2004). Target secondary structures sites can have a negative impact on gene knockdown since it changes the activation process of RISC complex and consequently it affects the mRNA cleavage (Birmingham et al., 2007).

The most important factor is the instability of the antisense strand 5' end, however there are some cases in which this property by itself does not provide a functional siRNA. Therefore, it is also important to consider the other aspects mentioned (Birmingham et al., 2007).

The siRNA sequence can be chemically synthetized with appropriated ribonucleioside phosphoramidites and a conversional synthesizer (Jackson & Linsley, 2010).

### 1.3.3 siRNA delivery methods

As previously referred, to activate the RNAi pathway, the siRNA must be inside the targeted cells cytoplasm. In some studies, it was proven that when the siRNA is delivered locally a significant knockdown on the targeted genes is observed, specifically, on the inhibition of respiratory viruses (Bitko, Musiyenko,

Shulyayeva, & Barik, 2005) and attenuating striatal and cortical neuropathology (Hofmann, Russell, Goldstein, & Brown, 1987).

On the other hand, systemic administration of naked siRNAs is not efficient due to phagocytose, serum proteins aggregation, easy degradation by endogenous nucleases, recognition by the immune system and fast renal clearance before entering in the targeted cell cytoplasm. In normal pH conditions, the siRNA sequence is negatively charged, as well as the targeted cell membrane, thus repelling each other. If the siRNA is able to enter the cell by endocytosis, then it is also necessary a fast escape from the endosome because it could be degraded. Regarding all these obstacles and others that may exist, it is expected less than 1% of the siRNA internalization (Ahmadzada, Reid, & McKenzie, 2018; Karim et al., 2018).

Consequently, through the years, several delivery systems have been engineered aiming to protect and improve the siRNA gene silencing. To design a siRNA nanocarrier, size, shape and surface charge are crucial aspects that must be considered. Renal filtration cut-off is about 50 kDa. Hence, to avoid renal clearance the siRNA delivery system should be bigger than 50 kDa, which corresponds to 5 to 6 nm. At the same time, particles with more than 100 nm in diameter will suffer phagocytosis. Therefore, the siRNA nanocarrier size should be between 5 and 100 nm. The nanocarrier shape has been a controversial subject because different studies came up with different conclusions (Majzoub, Ewert, & Safinya, 2016; Rezvani Amin, Rahimizadeh, Eshghi, Dehshahri, & Ramezani, 2013). The surface charge is one of the most important factors. Particles with different charges are more likely attracted. Therefore, since the cell membrane has anionic charge, the most cationic the nanoparticle is, the better (Ahmadzada et al., 2018).

Delivery systems can be divided in two categories: viral vectors and non-viral vectors (Ahmadzada et al., 2018; Kim & Eberwine, 2010).

Viral vectors comprise about 69% of all human trials for cancer-related gene therapies (Veenstra & Krauss, 2018). Viral vectors such as retro-virus, adenovirus and adeno associated virus are characterized for their high specificity, high gene expression efficiency and lack of replication and pathogenicity (Ferreira & Martins, 2017). However, this is not the best approach because these particles are potentially carcinogenic, can activate the immune system and have a high treatment cost associated (Karim et al., 2018; McNaughton, Cronican, Thompson, & Liu, 2009). On the other hand, non-viral vectors are a good alternative due to their non-immunogenic behavior, biological compatibility, higher specificity and lower production cost. The non-viral vectors can be divided in two categories: organic and inorganic (Karim et al., 2018; You et al., 2016). Both non-viral vectors may be surface modified for

example through PEGylation to escape the RES (reticuloendothelial system) and to renal clearance. Moreover, they can be coated with ligands or antibodies for specific delivery and to improve cellular uptake, and they can be coated with CPP (cell penetrating peptides) (Karim et al., 2018). Table 1, summarizes the siRNA based clinical trials for cancer therapy.

**Table 1** – siRNA-based clinical trials for cancer therapy and their status of development. (Adapted from (Karim et al., 2018)).

| Drug Formulation | Target Gene | Nanoparticle | Treatment | Diseases | Phase | Status |
|---|---|---|---|---|---|---|
| **DCR-MYC** | MYC | Lipid | siRNAs | Hepatocellular carcinoma | 1/2 | Ongoing; not recruiting; 2014-present |
| **DCR-MYC** | MYC | Lipid | siRNAs | Solid tumors, multiple myeloma, non-Hodgkin lymphoma or pancreatic neuroendocrine tumors | 1 | Ongoing; not recruiting; 2014-present |
| **ALN-VSP02** | KSP and VEGF | Lipid | siRNAs | Solid tumors | 1 | Completed |
| **Atu 027** | PKN3 | Lipid | siRNAs | Advanced cancers | 1 | Completed |
| **TKM-080301** | PLK1 | Lipid | siRNAs | Primary and secondary liver cancer | 1 | Completed |
| | PLK1 | Lipid | siRNAs | Neuroendocrine tumors | 1/2 | Completed |
| | PLK1 | Lipid | siRNAs | Advanced hepatocellular carcinoma | 1/2 | Completed |
| **siRNA-EphA2-DOPC** | EphA2 | Lipid | siRNAs | Advanced solid tumors | 1 | Recruiting |
| **siG12D-LODER** | KRAS | LODER polymer | siRNAs | Ductal adenocarcinoma or pancreatic cancer | 1 | Completed |
| **siG12D-LODER** | KRAS | LODER polymer | siRNAs | Pancreatic cancer | 2 | Not recruiting |
| **SNS01-T** | eIF5A | polyethyleneimine | siRNAs plasmids | Multiple myeloma | 1/2 | unknown |

### 1.3.4 siRNA transfection

Transfection is a procedure in which nucleic acids are introduced into the cells to produce genetically modified cells. Nucleic acid reagents, such as siRNAs are important tools to study mammalian cell structures, such as gene function and regulation (Kim & Eberwine, 2010; McNaughton et al., 2009). Basically, there are two types of transfection, stable and transient transfection. SiRNA knockdown relies on a transient transfection which is not integrated in the host cell genome and can be lost on cell division (Kim & Eberwine, 2010).

In an attempt to understand different organism's gene function, several transfection methods have been developed (Table 2). Depending on the cell type and experiment purposes, different approaches are used in each method. Ideally, the method used should have high transfection efficiency, low toxicity, minimal effects on normal physiology and be reproducible (Kim & Eberwine, 2010).

**Table 2** - Conventional transfection methods including biological, chemical and physical. (Taken from:(Kim & Eberwine, 2010)).

| Class | Methods | Advantages | Disadvantages |
|---|---|---|---|
| **Biological** | Virus – mediated | . High efficiency;<br>. Easy to use;<br>. Effective on dissociated cells, slices and in vivo. | . Potential hazard to laboratory personnel;<br>. Insertional mutagenesis;<br>. Immunogenicity;<br>. DNA package size limit. |
| **Chemical** | Cationic polymer | . No viral vector. | . Chemical toxicity to some cell types |
| | Calcium phosphate | . High efficiency. | . Variable transfection efficiency by cell type or condition. |
| | Cationic lipid | . Easy to use;<br>. Effective on dissociated cells and slices;<br>. Plenty of commercially available products;<br>. No package size limit. | . Hard to target specific cells. |
| **Physical** | Direct injection | . Simple principle and straightforward. | . Needs special instruments. |
| | Biolistic particle delivery | . Physical relocation of nucleic acids into cell. | . Vulnerable nucleic acids. |
| | Electroporation | . No need for vector | . Demands experimenter skill, laborious procedure |
| | Laser irradiation | . Less dependent on cell type and condition | |
| | Sonoporation | . Single cell transfection | |
| | Magnetic nanoparticle | | |

As previously mentioned, siRNAs are a viable alternative to chemotherapy in the fight against cancer. Cancer is a disease where multiple genes appear overexpressed. The aberrant regulation of MAPK pathway, in particular *MEK1* enhance the carcinogenesis due to their involvement in the regulation of cell proliferation and survival. Therefore, in this project a previously designed siRNA was used against *MEK1* gene to validate its potential for colon cancer therapy.

# 2. MATERIALS AND METHODS

## 2.1 Cell Culture

The human colon carcinoma cell line RKO (ATCC® CRL-2577™), HCT 116 (ATCC® CCL-247™) and HCT-15 (ATCC® CCL-225™) were kindly provided by CBMA (Central of Molecular and Environmental Biology-University of Minho). The human colon carcinoma cell line Caco-2 (ATCC® HTB-37™) was kindly provided by Dr. Mariana Henriques from the CEB (Centre of Biological Engineering-University of Minho) and the normal colon cell line CCD-841-CoN (ATCC® CRL-1790™) was purchased from ATCC. RKO, Caco-2 and CCD-841-CoN were grown in DMEM medium (Dulbecco Modified Eagle Medium) [Biochrom] supplemented with 10% (v/v) FBS (Fetal Bovine Serum) [Biochrom] and 1% (v/v) zell shield [Biochrom]. HCT 116 and HCT-15 were grown in RPMI medium (Roswell Park Memorial Institute) [Biochrom] supplemented with 1% (v/v) zell shield and 6% and 10% (v/v) FBS, respectively. The cell lines were maintained in a humidified incubator [Hera Cell] at 37°C and 5% $CO_2$. After reaching about 80% confluence, the cells were washed with PBS 1X (Phosphate Buffered Saline: 137 mM Sodium Chloride [Panreac], 10 nM Sodium Phosphate Dibasic [Scharlau], 2.7 nM Potassium Chloride [AppliChem] and Potassium Phosphate Monobasic [Riedel de Haën]) and detached using Trypsin/EDTA (0.05%/0.02% (w/v)) (Ethylenediaminetetraacetic acid) [Biochrom]. Sub-culturing was performed routinely. Cell culture experiments were performed in a Scanlaf Mars flow chamber [Labogene].

### 2.1.1 Cell line selection

To select the cell line to be further used in this work, RKO, HCT 116, HCT-15, Caco-2 and CCD-841-CoN cell lysates were submitted to a Western Blot procedure as explained in section 2.3., which allowed selecting the one with higher expression of the *MEK1* gene.

## 2.2 siRNA transfection

For the siRNA transfection procedure, a cationic liposome formulation was used (Lipofectamine RNAiMax Reagent [Invitrogen]). This technique enables the knockdown or even knockout of specific genes and allows studying their role and effects in the pathways in which they are involved.

To determine the *MEK1* gene knockdown effects on the RKO phenotype and in the downstream genes in the MAPK pathway, Western Blot experiments, qRT-PCR (reverse transcription polymerase chain reaction) assays, cell cycle analysis and proliferation assays were performed.

### 2.2.1 siRNA sequences

The siRNA sequences used for transfection were previously designed and purchased from IDT (Integrated DNA Technologies). The sequences targeting MEK1 gene (MEK1_siRNA), NC_siRNA (Negative Control siRNA) and Ty563-labelled siRNA used are the following:

- MEK1_siRNA:

5' – GGAUUACAUAGUCAACGAGCCUCCT – 3' – AACCUAAUGUAUCAGUUGCUCGGAGGA – 5'

- NC_siRNA

5' – CGUUAAUCGCGUAUAAUACGCGUAT – 3' – CAGCAAUUAGCGCAUAUUAUGCGCAUA – 5'

- Ty563-labelled siRNA

5' – CCUUCCUCUCUUUCUCUCCCUUGUG – 3' – GGAAGGAGAGAAAGAGAGGGAACAC – 5'

### 2.2.2 siRNA concentration optimization

It is important to have a high efficiency of siRNA-lipopolymer complexes. The use of high concentrations of siRNA can lead to off-target effects and this limit of concentration can be distinct for different cell lines (Ki et al., 2010). Therefore, it is necessary to find out which is the minimum concentration of siRNA that shows the same uptake from RKO cells after 24 hours of transfection.

One day prior transfection, $2 \times 10^5$cells per well (previously optimized in order to provide 50% confluence in the following day) were seeded in a 6-well plate containing coverslips in each well and were incubated overnight at 37°C and 5% $CO_2$.

In the next day, different concentrations of Ty563-labelled siRNA were prepared to obtain the siRNA final concentration of 10 nM, 30 nM and 50 nM. For each transfection sample, Lipofectamine RNAiMax Reagent was diluted in Opti-MEM I [Gibco]. Then, the siRNA was also diluted in Opti-MEM I and further added to the previously prepared Lipofectamine mixture and incubated for 20 minutes at room temperature, in the dark.

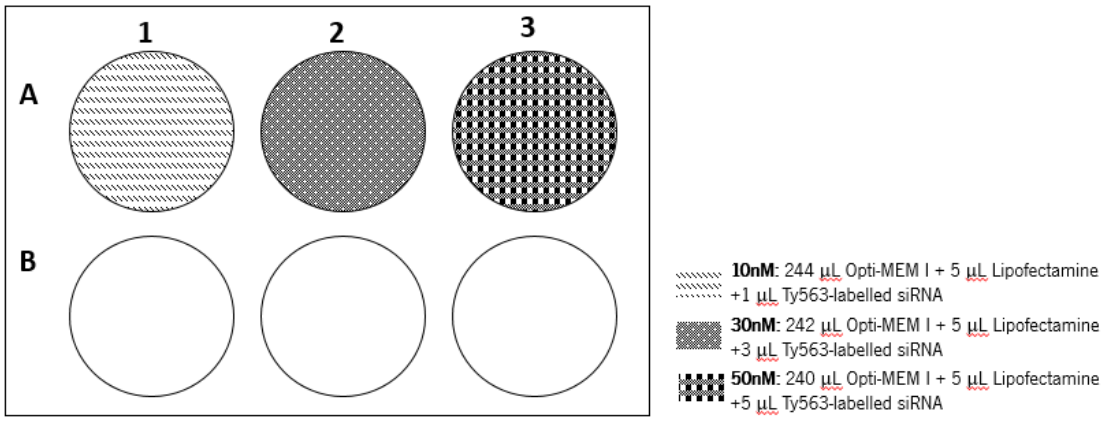


**Figure 4** - Composition of the mixtures with different concentrations used to transfect RKO cells with Ty563-labelled siRNA.

After incubation, about 250 µL of the mixtures were transferred to the wells according to Figure 4 and placed in the humidified incubator at 37°C and 5% $CO_2$, involved in aluminum foil. After 4 hours, 250 µL of 10% (v/v) FBS diluted Opti-MEM I (in the same proportion) were added to the wells.

In the next day of the experiment, the cells were washed twice with 500 µL of PBS 1X and then fixed in coverslips using 4% (w/v) of PFA (paraformaldehyde) in PBS 1X pH=7.4 for 40 minutes at room temperature. For actin staining, the cells were incubated with 100 µL of 0.1% (v/v) of Triton X-100 [Fisher Scientific] in PBS 1X for 5 minutes and washed twice with PBS 1X. Then, the cells were incubated in the dark for 20 minutes with 300 µL of PBS 1X supplemented with 1% BSA (Bovine Serum Albumin) and 3 µL of Alexa Fluor™ 488 Phalloidin [Molecular Probes]. Next, the cells were washed twice with PBS 1X. To stain the cells' nucleus, the cells were incubated in the dark for 30 minutes with DAPI (4',6-diamidino-2-phenylindole) [Biotium]. In the end, the cells were washed twice with PBS 1X, transferred to a slide and scanned on a Confocal Scanning Laser Microscope [Olympus BX61, Model FluoView 1000]. DAPI dye was used for detection of cell's nucleus (laser excitation line 405 nm and emissions filters BA 430-470, blue channel); Alexa Fluor™ 488 Phalloidin dye was used for actin detection (laser excitation line 488 nm and emissions filters BA 505–540, green channel) and Ty563-labbled siRNA (laser excitation line 559 nm and emissions filters BA 575–675, red channel). Images were acquired with the program FV10-Ver4.1.1.5 [Olympus].

### 2.2.3 MEK1_siRNA transfection

The siRNA of interest (MEK1_siRNA) was transfected into the cells as described in section 2.2.2 with some alterations. Briefly, in the first day four wells were seeded.

In the next day, the cells were transfected. Three of the wells correspond to the controls and one to the cells transfected with the MEK1_siRNA. The first well had only cells (cells), the second one had cells with the lipofectamine reagent (mock), the third well had cells transfected with the NC_siRNA (which is a siRNA proven to have no effect on cell proliferation, viability or morphology) and the last well had cells transfected with MEK1_siRNA. Different mixtures were prepared for each well, according to Figure 5. The medium was changed to complete medium in the next two days of experiment. Transfection images were obtained with an inverted microscope [LEICA DMIL] using a LEICA camera [CANON].

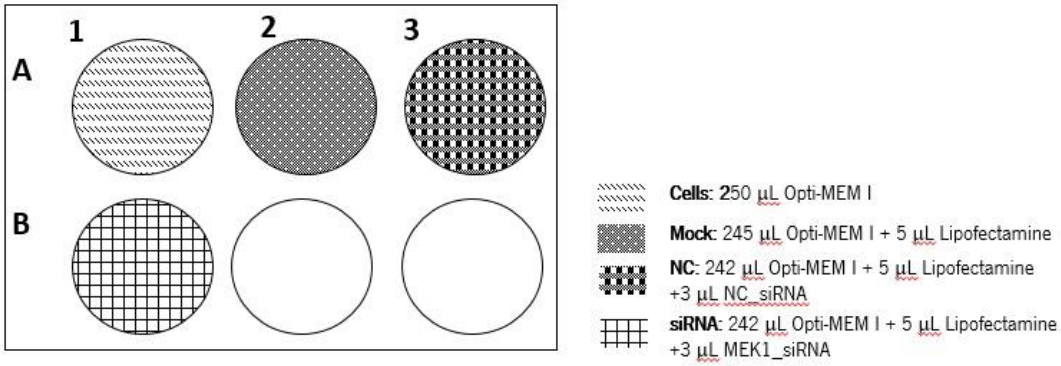


**Figure 5** - Representation of the mixtures used to transfect RKO cells with MEK1_siRNA.

## 2.3 Western Blot

### 2.3.1 Cell lysis

All steps of the cell lysis procedure were performed on ice. Initially, the media of the cells exposed to the same conditions were collected to a 15 mL falcon. Afterwards, the cells in the plate were washed with sterile PBS 1X at pH=7.4 at 37°C which was later transferred to the correspondent falcon.

In a second step of the procedure, the cells were detached with 500 µL of Trypsin-EDTA, resuspended with 2 mL of sterile PBS 1X at 4°C and added to the falcon. The cells in the plate were washed with PBS 1X at 4°C and were again transferred to the respective falcon. Then, the falcons were centrifuged [CL31R Multispeed – Thermo Scientific] at 2000 rpm, at 4°C for 10 minutes.

The supernatant was removed until it last just 500 μL of it and the pellet was resuspended and transferred to microcentrifuge tubes that were also maintained on ice. To each Eppendorf, 500 μL of PBS 1X at 4°C were added. These tubes were then centrifuged (1730R - ScanSpeed) at 2000 rpm at 4°C for 5 minutes and the supernatant discarded.

Afterwards, 200 μL of RIPA buffer (Radioimmunoprecipitation Assay Buffer: 150 mM sodium chloride [Panreac], 1% (v/v) NP - 40 (1% (v/v) Triton X-100, 150 mM Sodium Chloride [Panreac], 50 mM Tris-HCL pH=8 [Fisher Scientific], 0.5% (v/v) sodium dexycholate [Merck], 0.1% (w/v) SDS (Sodium Dodecyl Sulfate) [Fisher Scientific], 50 mM Sodium Floride [Sigma])) supplemented with 1% (v/v) Phosphatase Inhibitor (1 nM sodium orthovanadate [Sigma]) and 1% (v/v) Protease Inhibitor [Pierce] was added to the pellet. Then, these microcentrifuge tubes were settled on ice for 30 minutes, rocking the cells each 10 minutes and then centrifuged at 14000 rpm at 4°C for 15 minutes. In the end, the cell lysates were stored at -20°C.

The cell lysates protein quantification was measured using the BCA (bicinchoninic acid) protein assay kit [Fisher Scientific] according to the manufacturer's instructions, by measuring absorbance at 562 nm using 96-well plate reader (Synergy HT, BioTek) and Gen 5 software. The standard curve ($y = 0.0016x + 0.162$) μg/mL (Supplementary data A – BSA Calibration Curve) was determined using known concentrations of protein BSA.

### 2.3.2 SDS – PAGE

For the SDS – PAGE (Sodium Dodecyl Sulfate – PolyAcrylamide Gel Electrophoresis) procedure, a gel for protein separation was prepared on mini Mini-Protean Tetra System [Bio-Rad], according to the next table (Table 3).

**Table 3** - Necessary quantities (mL) of the different compounds to prepare SDS – PAGE gels (running and stacking gel).

| | Running gel (10%) (μL) | Stacking Gel (4%) (μL) |
|---|---|---|
| 40% (w/v) Acrylamide [Nzytech] | 750 | 200 |
| 1.5 M Tris-HCL pH=8.8 [Fisher Scientific] | 750 | - |
| 0.5 M Tris-HCL pH=6.8 [Fisher Scientific] | - | 500 |

| | Running gel (10%) (μL) | Stacking Gel (4%) (μL) |
|---|---|---|
| Ultrapure water | 2650 | 1175 |
| 10% (w/v) SDS [Fisher Scientific] | 60 | 20 |
| 0.1% (w/v) TEMED (Tetramethylethylenediamine) [Nzytech] | 3 | 1.5 |
| 10% (w/v) APS (ammonium persulfate) [VWR] | 200 | 100 |

Then, the cell lysates were diluted in a 1:1 ratio with Laemmli Sample Buffer 2X (65.8 mM Tris-HCl pH=6.8, 26.3% (w/v) Glycerol [Fisher Scientific], 2.1% (w/v) SDS, 0.01% (v/v) Bromophenol Blue [Fisher Scientific], 0.05% (v/v) 2-mercaptoethanol [Panreac]) and boiled at 95°C [Grant Bio Thermoshaker] for 5 minutes. Next, about 20 μg of each cell lysate was loaded into the wells and submitted to a two phase electrophoresis, starting at 60 V for 30 minutes and then 120 V for 60 minutes, both in TGS 1X (Tris - Glycine – SDS buffer: TGS 1X: 25 mM Tris-HCL at pH 8.6, 192 mM Glycine [Nzytech] and 0.1% (w/v) SDS). The gels were stained with Coomassie Blue stain (0.1% (v/v) Coomassie Brilliant Blue R-250 [Panreac], 50% (v/v) Methanol [Fisher Scientific] and 10% (v/v) Acetic Acid [Fisher Scientific]) and protein sizes were determined by comparing the migration of the protein band to a molecular mass standard.

### 2.3.3 Western Blot procedure

Proteins were transferred from the SDS gel without any staining to a nitrocellulose membrane [Amersham Protran] in cold transfer buffer (500 mM Glycine, 50 mM Tris-HCl, 20% (v/v) Methanol, 0,01% (w/v) SDS), performing a wet transference by “sandwiching” a sponge, blotting paper, membrane and the gel into a Mini Trans – Blot Cell [Bio-Rad], filled with cold transfer buffer, at 90 V for 90 minutes,

according to Figure 6 (Kurien & Scofield, 2006). The tank was placed in a stirring plate to allow a homogeneous buffer in the tank during the transference process.

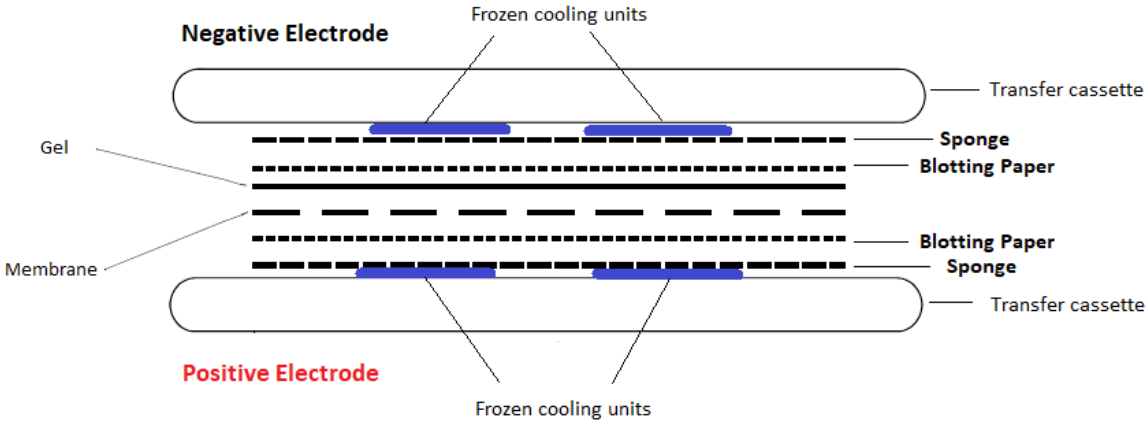


**Figure 6** - Mini Trans-Blot Cell Sandwich scheme. The transfer membrane and the gel are sandwiched between the blotting paper and the sponge. There are also represented frozen cooling units (Adapted from (Kurien & Scofield, 2006)).

In the end of the transference, the membrane was washed three times with TBS T (Tris-buffered saline with Tween 20: 500 mM Tris-HCL, 150 nM NaCl (Sodium Chloride) [Panreac], 0.1% (v/v) Tween 20 [Sigma]) for 5 minutes and blocked with 5% (w/v) BSA [Nzytech] in TBS T for 30 minutes at 4°C under agitation.

Then, the membrane was exposed to the primary antibody anti-MEK1 Rabbit Ab [Cell Signaling] diluted in 5% (w/v) BSA in TBS T (1:2000) and incubated overnight at 4°C with gentle agitation. In the next day, the membrane was washed 3 times with TBS T for 5 minutes, incubated with the secondary antibody anti rabbit IgG, HRP linked Antibody [Cell Signaling] diluted in 5% (w/v) BSA in TBS T (1:3000) and washed again 3 times with TBS T for 5 minutes. Next, the bands were detected with a substrate for ECL (enhanced chemiluminescence) [Bio-Rad], using Chemi-Doc RS System [Bio Rad].

Afterwards, the membrane was subjected to a stripping procedure, starting with two incubations with Stripping Buffer at pH=2.2 (1.5% (w/v) Glycine, 0.1% (w/v) SDS) at room temperature for 20 minutes each. Later, the membrane was incubated twice with PBS 1X for 10 minutes and twice with TBS T for 5 minutes, both at room temperature.

In this phase, the membrane is ready to repeat the blocking stage procedure, using at this stage a control, known as an antibody to detect a "housekeeping protein", Beta Actin Rabbit Ab [Cell Signaling], specifically. In the end, the bands were detected ECL, using Chemi Doc x-RS System.

## 2.4 Cell cycle

Initially, a 6-well plate was seeded with $2 \times 10^5$ cells per well. In the next day, cells were transfected as described in section 2.2.3. Then, the cells were scrapped with the help of a cell scrapper and the cell suspension of each well was transferred to a 15 mL falcon. The wells were washed twice with PBS 1X at 4°C which was then collected to the respective 15 mL falcon. The tubes were centrifuged at 2007 rpm for 5 minutes and the supernatant discarded. The pellet was resuspended in 500 μL of PBS 1X at 4°C and the tubes were maintained on ice for 15 minutes.

Subsequently, the cells were fixed with 1.5 mL of ice cold (- 20°C) absolute ethanol [Fisher Chemicals]. The suspension was vortexed and kept on ice for 15 minutes. The tubes were later centrifuged at 2007 rpm for 5 minutes and the supernatant discard. The pellet was resuspended twice in PBS 1X at 4°C and centrifuged under the same conditions, leaving 500 μL in the last time point to resuspend the cells.

Afterwards, the cells were treated with 1 μL of RNase A (Ribonuclease A) [Thermo Fisher] stock solution (10 mg/mL), vortexed and incubated at 37°C for 15 minutes. Then, samples were stained with 25 μL of PI (Propidium Iodide) [Thermo Fisher] stain solution (1 mg/mL), vortexed and incubated at room temperature for at least 30 minutes. Then, the samples were analyzed on the EC800™ flow cytometer [Sony Biotechnology] counting at least 20000 events. The data were analyzed using FlowJo Analysis Software (Tree Star, Inc).

## 2.5 Proliferation Assays

### 2.5.1 SRB

One day prior to the transfection procedure, a 6-well plate was seeded with $2 \times 10^5$ cells per well. After 72 hours of transfection (section 2.2.3.), culture medium was removed from the wells and the wells were washed with PBS 1X. Then, the cells were fixed with 1 mL of a solution of 1% (v/v) ice cold acetic acid in methanol and incubated for 90 minutes at – 20°C. After the incubation period, the solution was discarded and the plate was placed in an incubator [Memmert] at 37°C for 15 minutes to dry. Cells were then stained with 1 mL of a solution of 0.5% (v/v) of SRB (Sulforhodamine B) [Sigma] (1 mL per well) and incubated at 37°C for 90 minutes. The SRB solution was discarded and the cells were gently washed

with 1% (v/v) acetic acid solution and allowed to dry at 37°C for 15 minutes. About 1 mL of Tris 10 nM was added to each well to dissolve the SRB attached to cell proteins, under agitation.

Then, 200 µL of each well was transferred to a 96 well-plate (5 measurements per condition) and absorbance was measured at 540 nm using 96-well plate reader with Gen 5 software.

### 2.5.2 MTS

For the MTS (3-(4,5-dimethylthiazol-2-yl)-5(3-carboxymethonyphenol)-2-(4-sulfophenyl)-2H-tetrazolium) assay, 4 wells were seeded per condition with a concentration of $1 \times 10^4$ $cells$ per well, previously optimized to have a 50% confluent 96-well plate in the next day (Figure 7 (a)). Then, cells were incubated in a humidified incubator at 37°C and 5% $CO_2$.

After 24 hours, the mixtures were prepared according to Figure 7 (b) and 10 µL of each one (in quadruplicate) was transferred to a 96 well-plate and incubated in a humidified incubator at 37°C and 5% $CO_2$. After 4 hours, the cells were supplemented with 25 µL of 10% (v/v) FBS diluted in Opti-MEM I in a 1:1 ratio. The medium was changed to complete medium for the next two days of experiment.

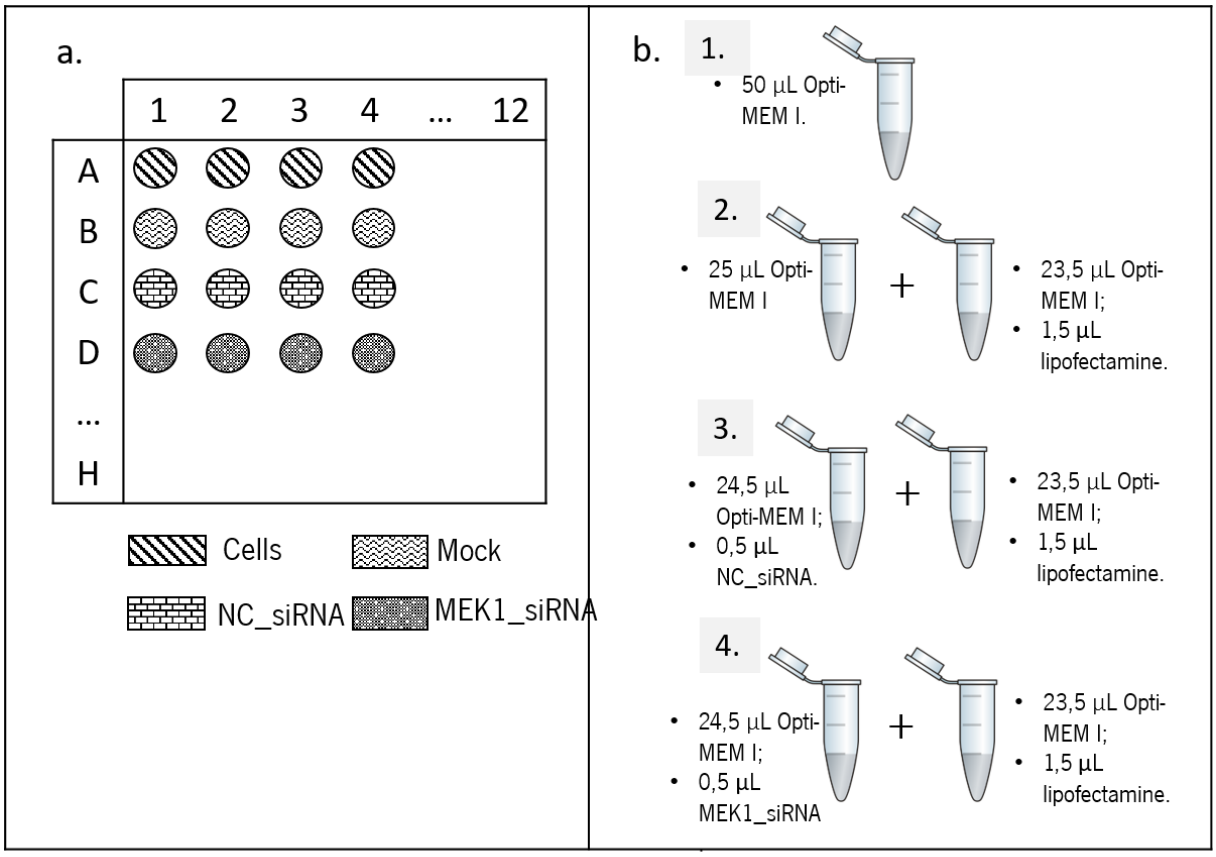


**Figure 7** – (a) Schematic representation of MTS assay conditions and (b) composition of the different mixtures prepared to transfect RKO cells. The mixtures 1., 2., 3. and 4. were transferred to the cells, Mock, NC and siRNA wells, respectively.

About 72 hours after transfection (section 2.2.3.), 20 µL of MTS reagent [Promega] it was added to each well. After 3 hours of incubation, using the previously mentioned conditions, the absorbance was measured at 490 nm using the 96-well plate reader with Gen 5 software. All the procedure was done in the dark and the 96-well plate was involved in aluminum foil.

## 2.6 qRT-PCR

### 2.6.1 Primers Design

Primers were designed using Primer3 design software available at http://bioinfo.ut.ee/primer3-0.4.0// (Table 4). To choose primers the settings defined in Table 4 were used.

**Table 4** - Primer3 settings chosen to design Primers.

| | | | | | | |
|---|---|---|---|---|---|---|
| **Product site ranges** | | 140-170 | | | | |
| **Number to return** | | 5 | **Max 3' stability** | 9 | | |
| **Max Repeat Mispriming** | | 12 | **Pair Max Repeat Mispriming** | 24 | | |
| **Max Template Mispriming** | | 12 | **Pair Max Template Mispriming** | 24 | | |
| **Primer size:** | **Min:** | 18 | **Opt:** | 20 | **Max:** | 27 |
| **Primer Tm:** | **Min:** | 59 | **Opt:** | - | **Max:** | 60 |
| **Max Tm Difference:** | | 0.3 | **Table of Thermodynamic Parameters:** | Breslauer at al. 1986 | | |
| **Primer CG%:** | **Min:** | 50 | **Opt:** | 55 | **Max:** | 60 |

After picking primer sequences, the BLAST (Basic Local Alignment Search Tool) search program (version BLAST+ 2.7.1) was used to verify the sequence specificity, available at https://blast.ncbi.nlm.nih.gov/Blast.cgi. The sequences chosen exhibited $p_{value}$<10.

Table 5 gathers the sequences of the designed primers used in this work.

**Table 5** - Sequences of the forward (FW) and reverse (RV) primers designed for the MEK1, ERK1 and GADPH (glyceraldehydes-3-phosphate dehydrogenase) genes.

| Primer | Sequence |
|---|---|
| MEK1.FW | GTT CAA GGT CTC CCA CAA GC |
| MEK1.RV | CGC TGT AGA ACG CAC CAT AG |
| ERK1.FW | AAG ATC AGC CCC TTC GAA CA |
| ERK1.RV | AGC CCA GCA ACA TCCTGT AT |
| GADPH.FW | GTC AGT GGT GGA CCT GAC CT |
| GADPH.RV | TCG CTG TTG AAG TCA GAG GA |

### 2.6.2 RNA extraction

Initially, RKO cells were seeded and transfected in 6-wells plate as described in section 2.2.3. RNA extraction was performed using a RNA extraction kit [Invitrogen] and following manufacturer's instructions. Briefly, after 72 hours of transfection, the cells were detached and the cell suspension corresponding to each well was transferred to the respective 1.5 mL RNA-free tube. Then, cells were centrifuged at 4015 rpm for 5 minutes at 4°C and the supernatant discarded.

The pellet was resuspended in 600 µL of Lysis Buffer with 1% (v/v) 2-mercaptoethanol [Panreac] by vortexing at high speed. To homogenize the sample, the lysate was passed 10 times through a 21-gauge needle attached to an RNase-free syringe.

Next, 600 µL of 70 % (v/v) ethanol was added to each cell homogenate and the tubes were vortexed in order to disperse any precipitate that may form.

Afterwards, the entire volume was transferred to the spin cartridge (with the collection tube) up to 700 µL of sample and then centrifuged at 9834 rpm for 15 seconds at room temperature. This step was repeated until all volume of the sample was processed and 700 µL of Wash Buffer was then added to the spin cartridge and centrifuged under the same conditions.

The collection tube was changed and 500 µL of Wash Buffer with ethanol was added to the spin cartridge and centrifuged again under the same conditions. This step was repeated and the spin cartridge was centrifuged at 9834 rpm for 2 minutes. Then, the spin cartridge was placed in a recovery tube and 50 µL of RNase-free water was added. The suspension was incubated at room temperature for one minute and the spin cartridge was centrifuged for 2 minutes at maximum speed. Finally, the purified RNA was quantified by NanoDrop 1000 Spectrophotometer [Thermo Scientific] and stored at -80 °C.

### 2.6.3 DNase treatment

DNase I, RNase-free supplied with $MnCl_2$ (1U/μL) kit [Thermo Scientific] was applied to the RNA samples in order to remove any residual DNA that might be contaminating them. Initially, a mixture with 1 μg of RNA extracted, 1 μL of 10X DNase buffer (100 mM Tris-HCl (pH 7.5 at 25 °C), 25 mM MgCl2, 1 mM CaCl2), 1 μL of DNase I and RNA-free water until 10 μL was prepared. This mixture was incubated at 37°C for 30 minutes. Later, 1 μL of 50 mM EDTA was added and incubated at 65°C for 10 minutes.

Afterwards, an agarose gel was performed in order to verify the RNA integrity. To prepare the 1% agarose gel, 1 g of agarose [Fisher Scientific] was dissolved in 50 mL of TAE (Tris-EDTA) 1X buffer [TAE 50X: 2 M Tris-HCL, 1 M acetic acid and 50 mM EDTA to pH 8.5] using a microwave at 500 W [Teka] and then 1.5 μL of Thiazole Orange [Sigma] was added. Gel electrophoresis was carried out at 90 V for 50 minutes in TAE 1X and the samples were loaded. In the end, Chemi Doc x-RS System was used to detect bands.

### 2.6.4 cDNA conversion

For random-primer cDNA reaction the iScript™ cDNA Synthesis kit [BioRad] was used and reverse transcription was performed according to manufacturer's instructions. Briefly, mixtures containing 4 μL of 5X iScript reaction mix, 2 μL of random primer, 1 μg of RNA sample, 1 μL of iScript reverse transcriptase and up to 20 μL of RNase-free water were incubated for 5 minutes at 25°C, for 30 minutes at 42°C and for 5 minutes at 85°C. Then, the cDNA was stored at -20°C.

### 2.6.5 qRT-PCR procedure

For qRT-PCR, it was necessary to set up standard curves for *MEK1*, *ERK1* genes and for *GADPH*, known as a housekeeping gene. Different cDNA template dilutions (1:20, 1:40, 1:80, 1:160, 1:320) were used with the set of primers previously designed (Table 5).

qRT-PCRwas performed using the SsoFast EvaGreen supermix [Bio-Rad] and following the manufacturer's instructions. Mixtures were prepared containing 5 μL of SsoFast™ EvaGreen® Supermix, the recommended primer concentration, 1 μL of cDNA and RNase/DNase free water up to 10 μL. Controls were also prepared, including a positive control using the housekeeping gene (GADPH), RNase/DNase free water as NTC (no template control) to verify any DNA contamination that may occur during reaction setup and NRT (no reverse transcriptase) to ascertain any genomic DNA contamination.

Amplification was conducted at 95°C for 30 seconds, then 39 cycles was performed at 95°C for 5 seconds and 60°C for 10 seconds in the Bio-Rad CFX96 Real-Time PCR Detection System. At the end, each melting curve was analyzed to confirm that the amplified product was specific.

## 2.7 Statistical Analysis

Statistical significance of the experimental results was determined by Two-way ANOVA with Tukey's multiple comparisons test using GraphPad Prism 7. For p-values below 0.05 the differences between experimental groups were considered significant.

# 3. RESULTS AND DISCUSSION

## 3.1 Cell line selection

*MEK1* (or *MAP2K1*) gene located upstream ERK-MAPK pathway is involved in cells proliferation, differentiation, transcription regulation and development. If *MEK1* is highly active, cells may suffer certain transformations including excessive proliferation such as what is observed in cancerous cells. Therefore, *MEK1* gene can be potentially used as target for cancer treatment (Oh et al., 2016).

The colon cancer cell line used in this work was chosen based on the cell line availability that exhibit the higher expression of the *MEK1* gene. For this, purpose it was cultured four different colon cancer cell lines (Caco-2, HCT 116, RKO and HCT-15) and one normal colon cell line (CCD-841-CoN). After preparing cell lysates from the different cell lines a Western Blot was performed (Figure 8).

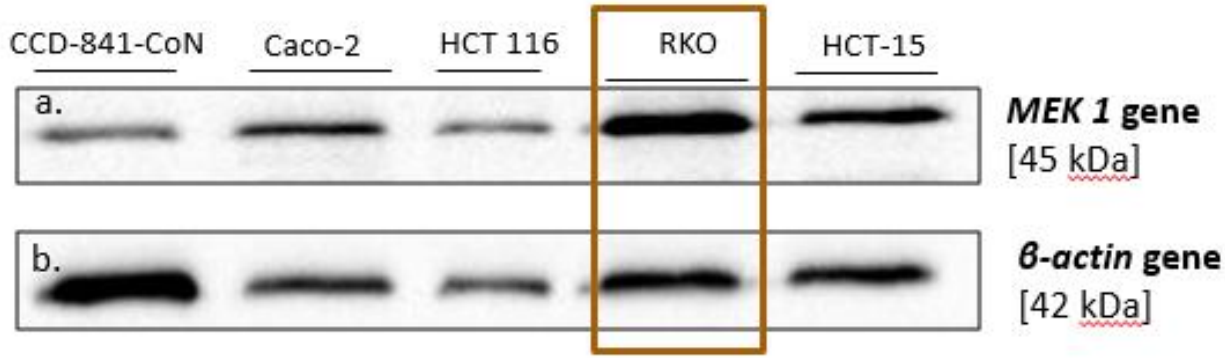


**Figure 8** - Western Blot results of comparative levels of expression of (a.) MEK1 [45 kDa] and (b.) β-actin [42 kDa] genes on CCD-841-CoN, Caco-2, HCT 116, RKO and HCT-15 cell lines. β-actin was used as a loading control.

The resultant bands represent the protein level of MEK1 and β-actin in each cell line. Thus, it was possible to determine the cell line with higher expression of the MEK1 gene when comparing with β-actin, which is a "housekeeping protein" that is expressed constantly and at high levels in all cell types.

The results normalization was performed through ImageJ software and, as the image suggests, the cell line with higher expression of the *MEK1* gene was the RKO cell line. This cell line exhibited a *MEK1* gene expression about 1.2 times higher than the second cell line with higher expression (HCT-15) as showed by the higher amount of protein that can be visualized, 1.4 times more than Caco-2, twice the amount of HCT 116 and 4.5 times more than the normal colon cell line (control).

The overexpression of the *MEK1* gene is commonly detected on several colorectal cell lines (Fang & Richardson, 2005; Urosevic et al., 2014), hence our results showed that the colon cancer cell line with lower expression of the *MEK*1 gene (HCT 116) expresses this gene 2 times more than the normal colon cell line CCD-841-CoN is in great agreement with previous studies.

## 3.2 siRNA transfection

In this work, a siRNA sequence was designed for targeting the *MEK1* gene. It is expected that the mRNA cleavage induced by the siRNA originates the knockdown or even knockout of our interest gene.

To accomplish this goal, the siRNA transference into RKO cells was performed through lipofection using Lipofectamine RNAiMAX Reagent. This reagent is able to form a transfection complex composed by the cationic lipid and the anionic nucleic acid which will merge with the cell membrane. As a result, this process leads to the siRNA delivery into the cell (Majzoub et al., 2016).

As previously mentioned, a special care must be given to the choice of the siRNA concentration used in the transfection experiments because high concentrations may induce off-target effects such as, for instance, unexpected cell phenotypes (Jackson & Linsley, 2010), dysregulation of other genes rather than the ones defined as targets or even the activation of the interferon response (Ki et al., 2010). One the other hand, low concentrations may have no effect on gene silencing. Thus, understanding which is the ideal siRNA concentration is crucial, more specifically, which is the optimum siRNA concentration to achieve the best transfection conditions. Therefore, the transfection efficiency was monitored using a fluorescent dye-labelled siRNA (Ty563-siRNA) and the images were obtained through confocal microscopy (Figure 9) using the same settings for all images.

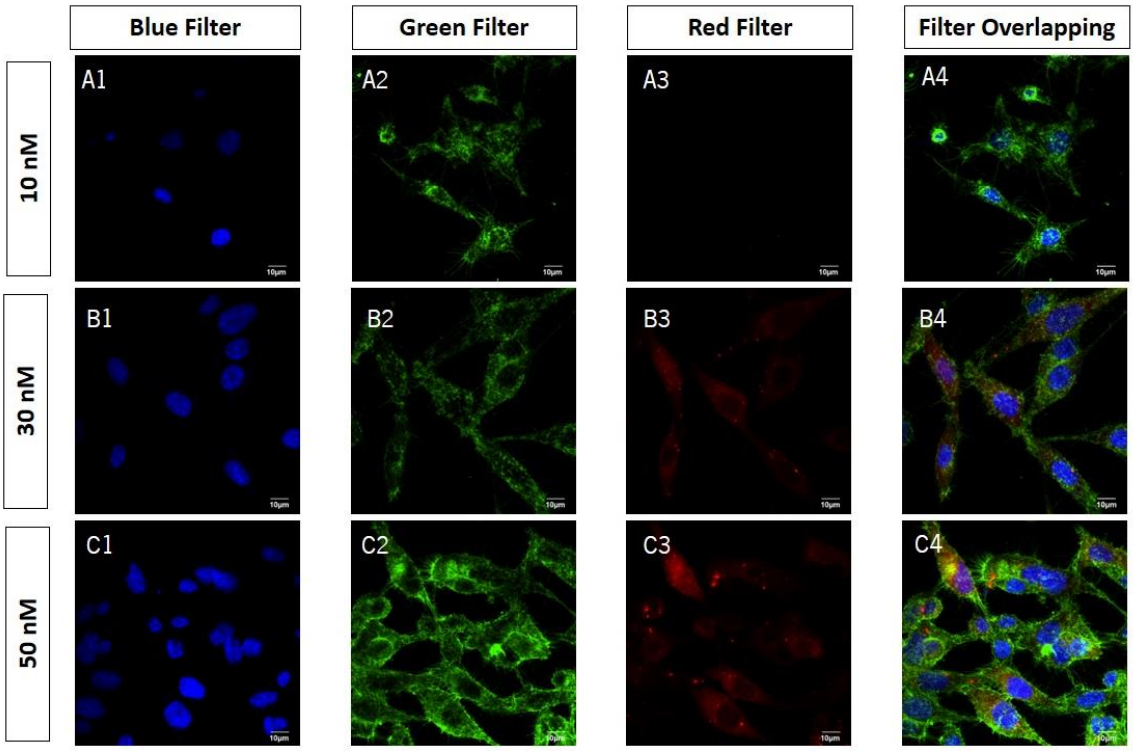


**Figure 9** - Internalization of different concentrations of Ty563-labelled siRNA by RKO cells (A-C). Images show RKO cells incubated with 10 nM (A1-A4), 30 nM (B1-B4) and 50 nM (C1-C4) of Ty563-labelled siRNA. (1) cell's nucleus stained with DAPI dye- Blue; (2) Actin stained with Alexa Fluor™ 488 Phalloidin dye- Green; (3) Ty563-labbled siRNA - Red and (4) Filters overlapping. Scale bars represent 10 µm.

From Figure 9 it is possible to see that with a 10 nM concentration of labelled-siRNA (A3) the cells showed little internalization of siRNA (represented by red dots). One the other hand, in the cells transfected with both 30 nM (B3) and 50 nM (C3) of labelled-siRNA the presence of red dots is clear, thus meaning that an efficient uptake of siRNA by the cells occurred. Indeed, between the cells transfected with 30 nM and 50 nM of siRNA there was almost no difference. This means that if we use 30 nM or 50 nM of siRNA the level of internalization by the cells will be similar. Therefore, to use the lower amount of siRNA necessary to transfect efficiently RKO cells, a 30 nM concentration was chosen.

Ki and his co-workers showed that a 20 nM siRNA concentration was enough to efficiently transfect astrocytes and microglial cells and that only a concentration higher than 80 nM could lead to off-target effects (Ki et al., 2010). Moreover, Schmitz and Chu performed a study on RKO cells with an siRNA different than the one used in this study and showed that the cytotoxic effects of siRNA were dose-dependent and that a siRNA concentration higher than 300 nM could lead to off-target effects (Schmitz & Chu, 2011). Based on these studies, it is probable that the changings observed on RKO cells, using a 30 nM siRNA concentration, are a direct consequence of the effects of the siRNA of interest on the *MEK1* gene silencing and not of any other cellular events.

One other interesting finding that can be noticed from Figure 9 is that mostly all the siRNA internalized by the cells is concentrated on the cytoplasm, which is an essential aspect for the specific gene silencing process effectiveness (Ahmadzada et al., 2018).

Afterwards, microscope images were acquired in order to observe which was the impact of the siRNA on cell proliferation and/or morphology among the tested conditions (Figure 10).

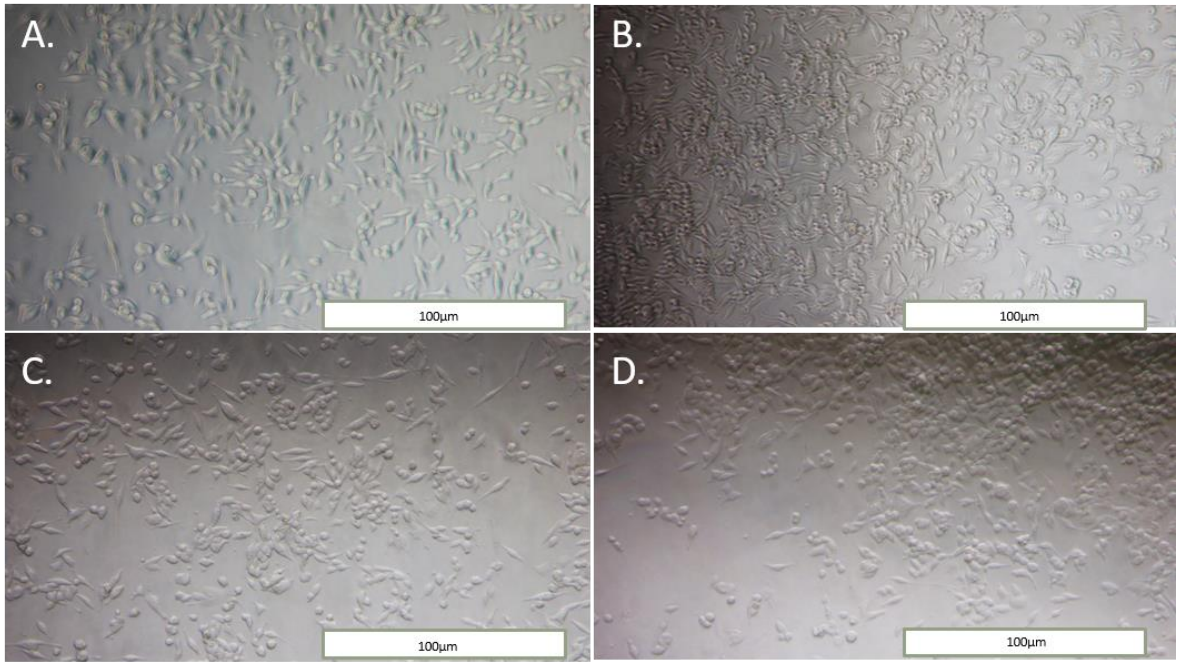


**Figure 10 -** Inverted microscope Leica DMIL images of RKO cells after 72 hours of transfection. (A.) RKO cells non-transfected, (B.) RKO cells treated only with Lipofectamine® RNAiMAx Reagent (Mock), (C.) RKO cells transfected with a negative control siRNA (NC_siRNA) and (D.) RKO cells transfected with 30 nM of the siRNA designed (MEK1_siRNA). The magnification used was 10X.

Figure 10 shows the differences, after 72 hours, of RKO cells under different conditions. It is possible to observe that the images of cells non-treated, cells treated with Lipofectamine® RNAiMax Reagent (mock) and cells transfected with NC_siRNA (a siRNA proven to have no effect on cell proliferation, viability or morphology) are similar in what regards proliferation and morphology. These results proved that any changes that may occur on the cells transfected with siRNA targeting MEK1 are just a siRNA consequence and not due to the transfection reagent or even due to an effect from a RNAi specific sequence.

Comparing the image of cells transfected with MEK1_siRNA with the controls, it is possible to observe an apparently diminution on the number of cells, meaning a decrease of cell proliferation. As previously referred, the *MEK1* gene belongs to the MAPK pathway, known to be involved on cell proliferation (Fang & Richardson, 2005). On the other hand, we can also see that the cells transfected with MEK1_siRNA have a slightly rounder shape than the controls which exhibit an elongated shape. This usually happens when the cell adhesion is affected and, consequently, cell detachment occurs. Therefore, to understand those events additional specific experiments, such as SRB, MTS and cell cycle analysis should be performed.

## 3.3 Cell Cycle

MAPK pathway is deeply involved in the regulation of apoptosis, cell cycle regulation and differentiation. Changes on some proteins present on MAPK (such as MEK1) lead to modifications on the expression of some molecules ($p16^{Ink4a}$, $p15^{Ink4b}$ e $p21^{Cip1}$) that regulate the cell cycle (McCubrey et al., 2007).

To learn about MEK1_siRNA effects on the cell cycle, RKO cells were stained with propidium iodide and their fluorescence were quantified using flow cytometry (Figure 11).

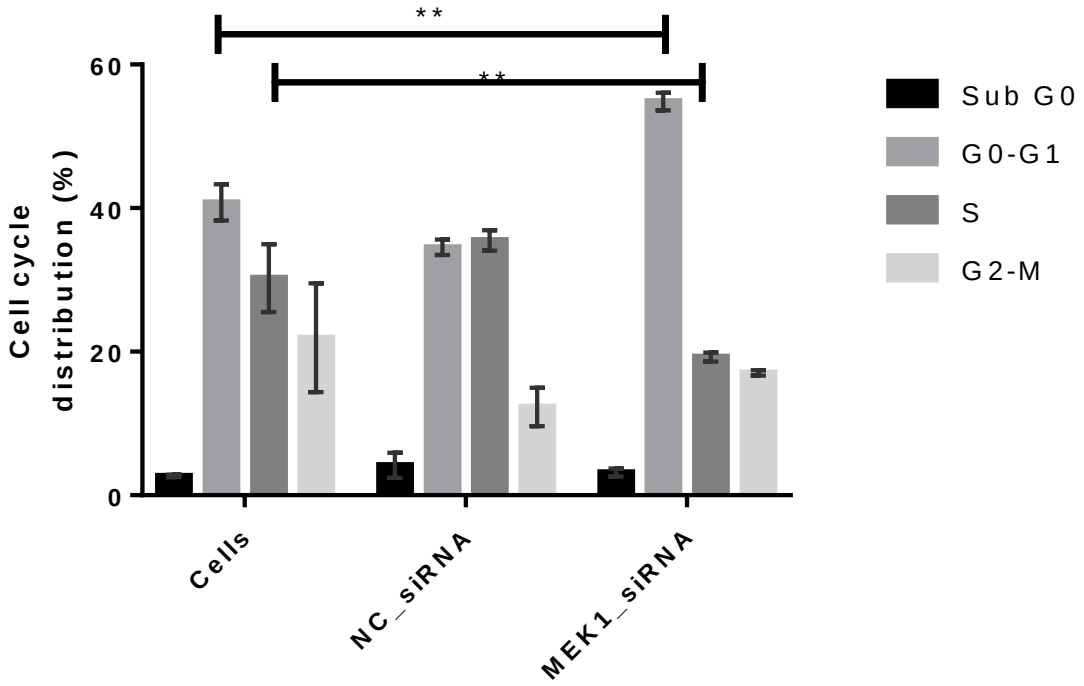


**Figure 11 -** RKO cell cycle after 72 hours of incubation of not transfected (cells), transfected with NC_siRNA and transfected with MEK1_siRNA. Cell cycle was analyzed through Flow Cytometry. Data was analyzed by two-way ANOVA with Tukey's multiple comparisons test using GraphPad Prism 7 (** 0.001< p-value < 0.01).

From Figure 11 it is possible to conclude that between the controls (non-treated cells and cells transfected with NC_siRNA) there was no significant difference in each cell cycle phase. Moreover, a significant difference was observed between the controls and the cells transfected with MEK1_siRNA. Specifically, a higher percentage of cells transfected with MEK1_siRNA on G0-G1 phase was observed. This means that the *MEK1* gene knockdown induces a cell cycle arrest on G0-G1 phase preventing cells to enter the S phase. The hypothesis of the cell cycle arrest is also enhanced by the significant decreased of the percentage of cells transfected with MEK1_siRNA on S phase when comparing with the controls. Thus, the cell proliferation has been probably affected since the DNA replication occurs in S phase

(Schafer, 1998). Those results were expected since a proliferation decrease could be visually observed on the microscope images.

Villanueva and co-workers showed that the inhibition of *MEK1* on human melanoma cell lines was also translated into a G0-G1 cell cycle arrest (Villanueva et al., 2010). Moreover, according to McCubrey the changes that some *MEK1* downstream molecules suffered can lead to a premature G0-G1 cell cycle arrest and eventually to a consequent cell senescence (McCubrey et al., 2007). *MEK1* is considered a good target for cell cycle arrest on tumor cells (Menges & McCance, 2008)

To observe the practical effect of *MEK1* knockdown on cell proliferation, two cell proliferation assays were performed (SRB and MTS).

## 3.4 Proliferation assays

### 3.4.1 SRB

The SRB experiment is used to assay the *in vitro* cytotoxicity as it is able to measure cell proliferation and viability. This is a quantitative method that measures the total protein content (Balko, Jones, Coakley, & Black, 2009). The results of the SRB assays performed on RKO cells under different conditions are illustrated on Figure 12.

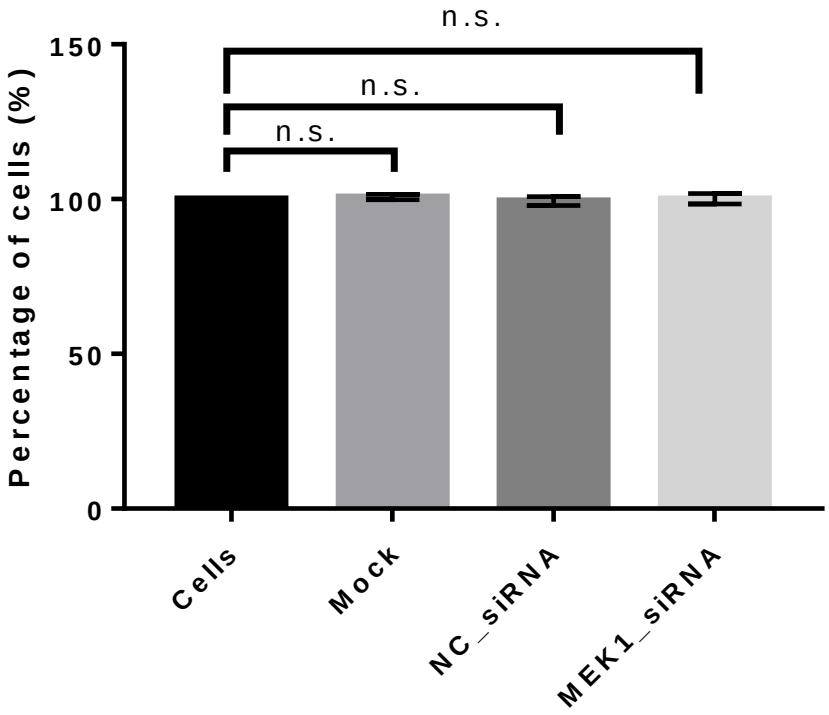


**Figure 12** - SRB assay on RKO cells, RKO cells treated only with Lipofectamine RNAiMax Reagent (mock), RKO cells transfected with NC_siRNA and RKO cells transfected with MEK1_siRNA after 72 hours of incubation. Results analyzed by two-way ANOVA with Tukey's multiple comparisons test using GraphPad Prism 7 (ns p-value ≥ 0,05).

Regarding SRB experiments, some studies have reported that the inhibition/knockdown of *MEK1* gene could lead to a decrease of cell proliferation on cancer cells (Balko et al., 2009; Oh et al., 2016). However, our SRB results suggested that the knockdown of the *MEK1* gene on RKO cells does not have any meaningfully effect on cell proliferation, since the percentage of cells remain approximately the same in all conditions. However, the previous experiments suggested that the cell proliferation decrease was a consequence of *MEK1* gene knockdown.

It is important to notice that the SRB experiment is a precise method but, as mentioned before, it only quantifies the protein content. Therefore, it is possible that during the experiment time period we do not observe a decrease on the number of cells but only a loss of their proper function, such as the ability of adhesion (previously observed) or even metabolic defects. Therefore, to have more information on the cells proliferative behavior a MTS assay was performed.

### 3.4.2 MTS

The MTS assay is also a colorimetric assay like the SRB but it measures the mitochondrial activity on metabolically active cells (viable cells) (Fujihara, Kotaki, & Ramakrishna, 2005). The MTS tetrazolium is reduced by NAD(P)H-dependent dehydrogenase enzymes in metabolic active cells. Therefore, the number of metabolic active cells is directly proportional to the medium color intensity.

To perform the MTS assay, the transfection conditions were optimized to a 96-well plate and the data was obtained through absorbance measurement (Figure 13).

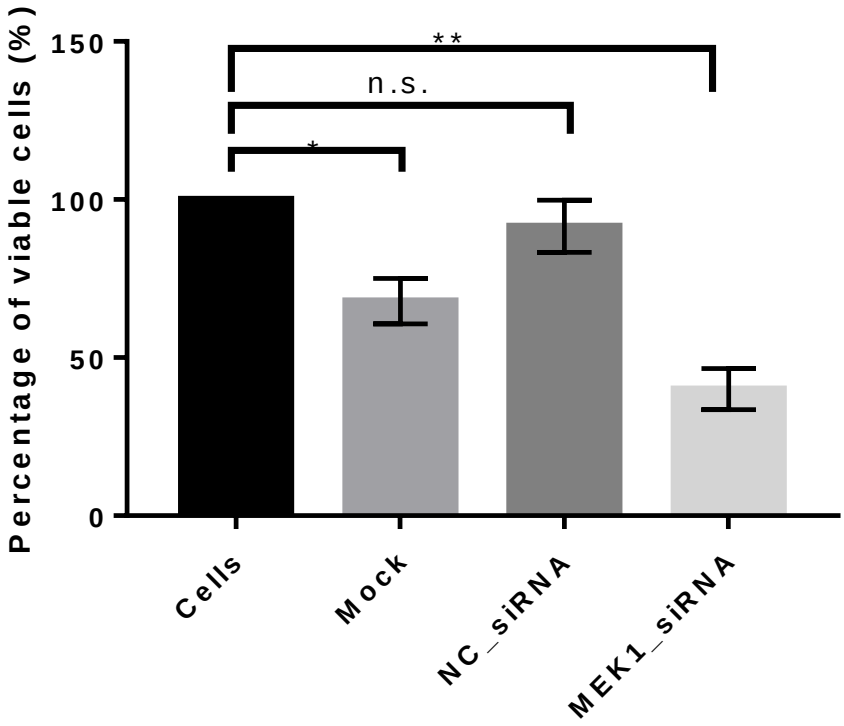


**Figure 13 -** MTS assay on RKO cells, RKO cells treated only with Lipofectamine RNAiMax Reagent (mock), RKO cells transfected with NC_siRNA and RKO cells transfected with MEK1_siRNA after 72 hours of incubation. Results analyzed by two-way ANOVA with Tukey's multiple comparisons test using GraphPad Prism 7 (ns p-value $\geq$ 0,05; * 0.01< p-value < 0.05; ** 0.001< p-value < 0.01).

Regarding the controls on Figure 13, it can be seen that the percentage of viable cells on the wells treated only with Lipofectamine® RNAiMax Reagent was a slightly different from the other controls. This was not an expected result because this reagent is proven to have no effect on the cells, only helping the transfection process. Thus, from this observation we can conclude that those cells suffered some kind of stress during their manipulation. Another explanation could lie on the fact that the MTS is an assay with high variability between assays (as it is possible to see from the standard deviations) which could

ultimately influence the results. Moreover, the lipoplex is positively charged whereas the cell membrane components are negatively charged. Since the lipoplex does not possesses any negative charge inside, it may develop an electrostatic interaction with the cell membrane causing cell membrane disruption and damage (Rezvani Amin et al., 2013).

Comparing the cells transfected with MEK1_siRNA with the controls it is possible to observe a significant decrease on cell viability. Those results are corroborated by the cell cycle results, which indicated a cell cycle arrest on G0-G1 phase. It is known that when the cell cycle stops at the G0 checkpoint cells remain in a quiescent state, i.e., they are still alive but just not with metabolically active (Schafer, 1998), which explains the fact that SRB results show that the number of cells (protein content) remains the same during the experiment and MTS results show a decrease on the MEK1_siRNA transfected cells viability.

Maybe if the experimental period was extended, a pronounced cell viability decrease on MEK1_siRNA transfected cells could be observed through SRB, as we have seen that the cells adhesion ability is compromised. Mammalian cells need to be adhered to a surface to be able to grow so, after a few more days they would die.

## 3.5 Western Blot

To access the level of MEK1 knockdown on RKO cells transfected with MEK1_siRNA a western blot experiment was performed and the same controls were used. The membrane where the cell lysates were transferred to was exposed to the anti-MEK1 antibody and, after a striping procedure, the anti β-actin antibody, enabling us to access the level of knockdown of the MEK1 protein on the transfected cells (Figure 14).

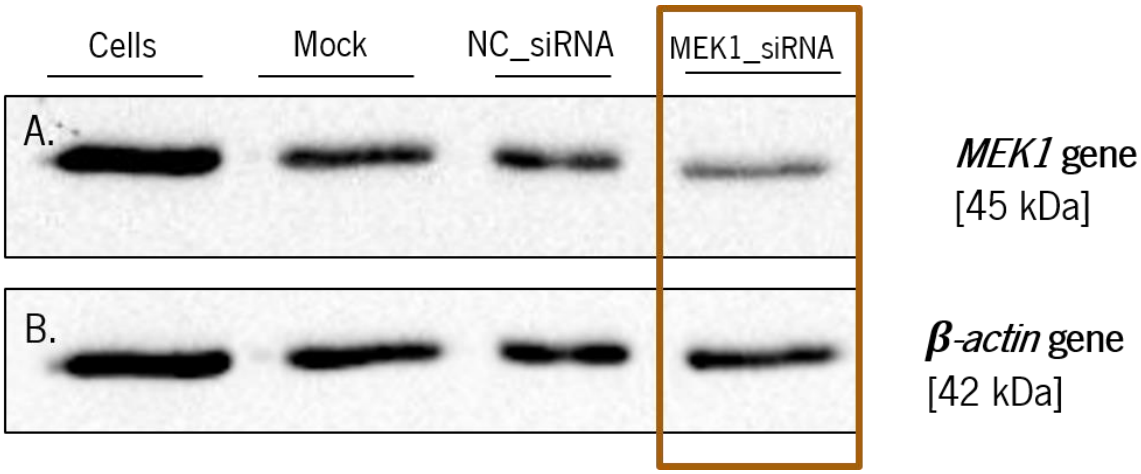


**Figure 14 -** Western Blot results of comparative levels of expression of (a.) MEK1 [45 kDa] and (b.) β-actin [42 kDa], after 72 hours of transfection on RKO cell line. B-actin was used as a loading control.

β-actin is used as a loading control because it is expressed constantly and at high levels in all cell types. On Figure 14 it is possible to observe, in each control (mock and NC_siRNA), a similarity of the band intensity between MEK1 and β-actin which means that the *MEK1* gene level of expression is not meaningfully affected. However, a difference is noticed on the MEK1_siRNA exposed to the anti-MEK1 antibody. Bands were quantified using ImageJ software and were expressed as integrated intensity of bands (band area × relative intensity). It was estimated that the cells transfected with MEK1_siRNA suffered a 52.5% MEK1 knockdown at a protein level, meaning that the MEK1_siRNA was able to target the MEK1 specific mRNA and eliminate part of it.

Western Blot is a unique procedure for protein immunodetection with several advantages such as the possibility of storage protein patterns for a long period of time, as well as to have multiple gel replicas (Kurien & Scofield, 2006). Nevertheless, there is an important drawback which lies on the fact that this is a semi-quantitative procedure, providing a relative comparison between protein levels. Therefore, to have an absolute measure of the gene knockdown a qRT-PCR should be performed.

## 3.6 qRT-PCR

qRT-PCR is a procedure that monitors the amplification of a targeted DNA molecule in real time. The total RNA was extracted from all the controls conditions (cells, mock and NC_siRNA) and from the RKO cells transfected with MEK1_siRNA. Then, the RNA sample of each condition was treated with DNase I to eliminate any DNA residues that may still be present.

Each RNA sample was quantified by NanoDrop 1000 spectrophotometer and the concentrations obtained were considered acceptable. This equipment also enables the assessment of sample quality through absorbance measurements at 230 nm, 260 nm and 280 nm. Usually, RNA samples considered pure yield a 260/280 ratio of approximately 2 and a 260/230 ratio in the range of 1.8 – 2.2. In this work a 260/280 ratio of about 2 was always verified, thus implying pure RNA samples. However, the 260/230 ratio for the same samples was lower than the previously mentioned range. Therefore, it is possible that contaminants that absorb at 230 nm, such as EDTA, carbohydrates and phenol, may be present (Desjardins & Conklin, 2010). To have further knowledge on the quality of RNA samples, an agarose gel was performed (Figure 15).

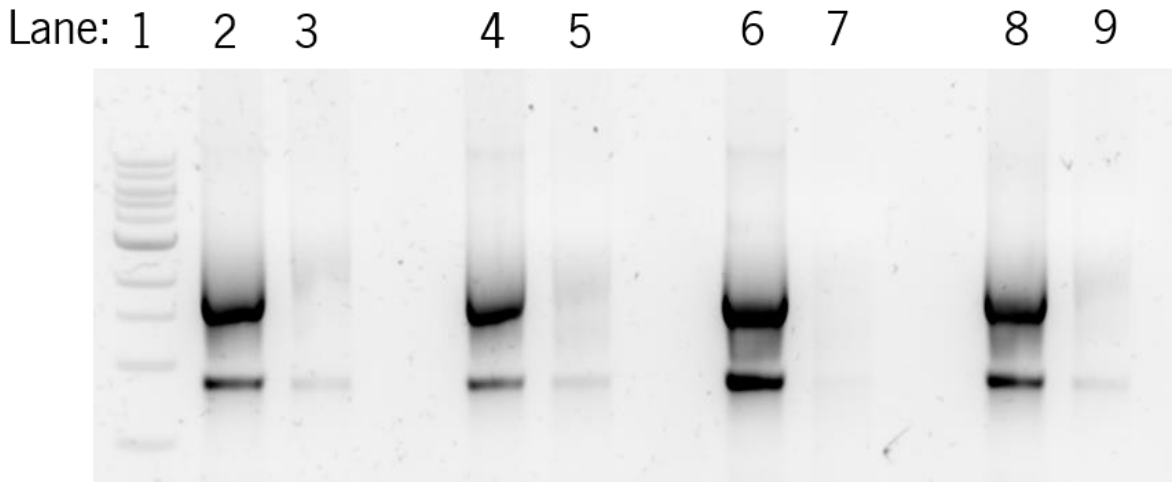


**Figure 15 -** Agarose gel (1%) of total RNA extraction (Lane 2,4,6,8) and correspondent Dnase I-treated RNA (Lane 3,5,7,9) samples of RKO cells after 72 hours of transfection. Lane 1: 1 kb DNA ladder. Total RNA of Lane 2: non-transfected cells (RNA_cells); Lane 3: non-transfected cells treated with DNase I (DNase_cells); Lane 4: cells treated only with Lipofectamine®RNAiMAX Reagent (RNA_mock); Lane 5: cells treated only with Lipofectamine®RNAiMAX Reagent and DNase I (DNase_mock); Lane 6: cells transfected with a negative control siRNA (RNA_NC); Lane 7: cells transfected with a negative control siRNA (DNase_NC) and treated with a DNase I; Lane 8: cells transfected with MEK1_siRNA (RNA_siRNA) and Lane 9: cells transfected with MEK1_siRNA (DNase_siRNA) and treated with a DNase I.

The quality of eukaryotic RNA can be inferred by the presence of three distinct bands. The first top band represents the 28S rRNA (ribosomal RNA) and the middle corresponds to 18S RNA. An intensity ratio of 2:1 between 28S:18S band is also an indicator of high RNA quality, which is apparently observed for each condition lane (Fleige & Pfaffl, 2006).

Figure 15 also shows samples of each condition treated with DNase I (Lane3: DNase_cells, Lane 5: DNase_mock, Lane 7: DNase_NC and Lane9: DNase_siRNA). It is predictable that these lanes are similar to the correspondent total RNA lanes but with less intensity. This is true for all conditions except for DNase_NC, meaning that this sample was degraded during the process. Therefore, the RNA_NC treatment with DNase was repeated and a new agarose gel was performed (Figure 16).

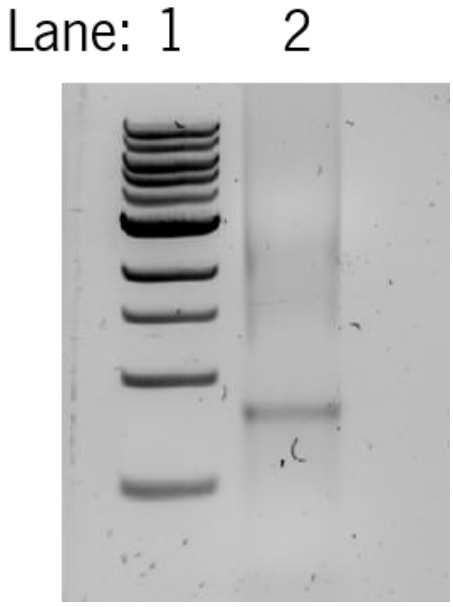


**Figure 16 -** Agarose gel (1%) of DNase I treated samples of RKO cells after 72 hours of transfection. Lane 1: 1 kb DNA ladder. Lane 2: cells transfected with a negative control siRNA (DNase_NC) and treated with a DNase I.

After having all RNA preparations treated with DNase I, they were converted to cDNA and were ready to be used for qRT-PCR.

Regarding the MAPK pathway, it is possible to realize that there are some important genes located downstream *MEK1* gene that could explain some of the proliferation/migration events. It is known that two of those genes are the *WAVE-2* (Wiskott-Aldrich syndrome protein family member 2) and *ERK1* genes and that they are directly involved in cell migration and in cell adhesion, respectively (Fang & Richardson, 2005). Therefore, to better understand the consequences of the *MEK1* gene knockdown, the silencing level of *ERK1* gene was quantified. Figure 17 comprises the silencing level of *MEK1* and *ERK1* genes on cells transfected with siRNA_MEK1 on cells transfected with NC_siRNA. Unfortunately, the *WAVE-2* gene knockdown could not be evaluated within the duration of this work due to time restrictions.

Initially, calibration standard and melt curves for the *GADPH* (housekeeping gene), *MEK1* and *ERK1* genes (Supplementary Data B) were established. Standard curves are usually prepared for PCR reaction standardizing to understand, for example, if the primers and the template concentration are good for reaction. At the same, it is possible to calculate the primers efficiency which has high relevance in real time PCR reactions. Basically, these curves should have an efficiency between 90 and 110% (Broeders et al., 2014) and in this work, it were achieved 103.3%, 104.2% and 108.3% efficiencies for *GADPH*, *MEK1* and *ERK1* curves, respectively. Furthermore, *MEK1* standard curve had good $R^2$ values

(0.992), however for *GADPH* and *ERK1* standard curves, $R^2$ value (0.943 and 0.971, correspondingly) were not good enough maybe due to possible pipetting technique errors.

Additionally, melting curves allow to check if the primers are giving a specific PCR product and if there is a nonspecific amplification. In a melting curve of a specific amplification we should have only one peek. Moreover, melting curves are important for checking if RNA samples are contaminated with genomic DNA, if there are extra sequences between primers and also if primer-dimer is affecting the assays (Gajadhar, Reyes, & Lalonde, 2013). In this work, for all the generated melting curves were observed that independently of the dilution template, each melting curve had the same peek.

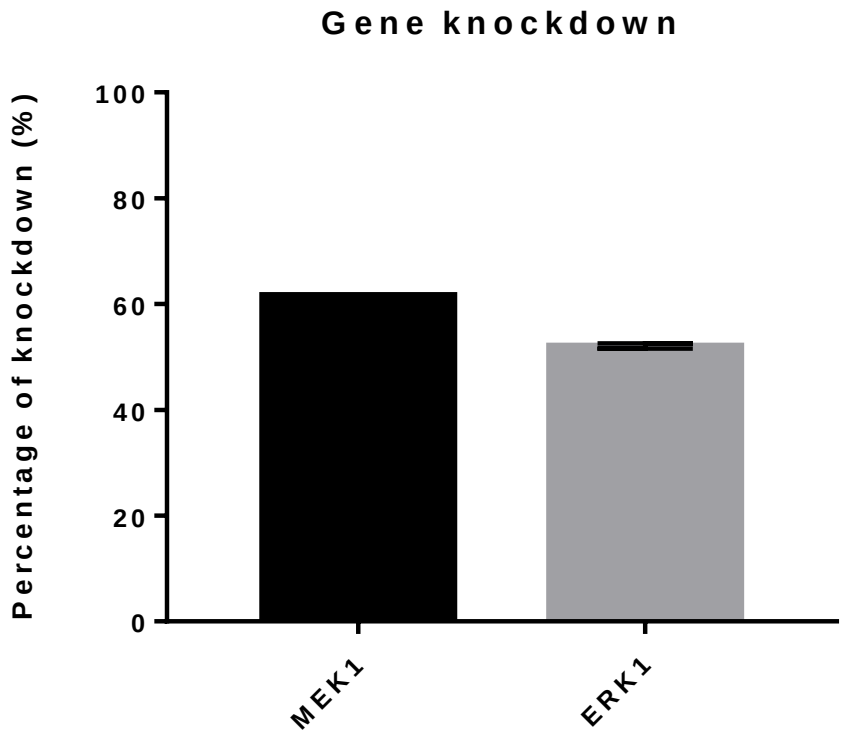


**Figure 17** - Gene knockdown on RKO cells 72 hours after transfection, quantified through qRT-PCR. Evaluation of MEK1 silencing and consequent effect on ERK1 downstream located gene. The data were normalized to GADPH levels and are represented as mean ± S.D.

From Figure 17, it is possible to confirm that the transfection procedure was efficient. The transfection of RKO cells with the siRNA that targets the *MEK1* gene leads to a mRNA silencing level of 61.6% of this gene in particular. These results confirm the ones regarding the assessment of the protein expression, since the Western Blot results also show a decrease of the protein expression level (52.5%). A knockdown at the protein level not accompanied by a knockdown at a mRNA level could indicate that other mechanism rather than siRNA transfection was present (Mocellin & Provenzano, 2004).

Sahin and co-workers designed several siRNAs targeting different genes for breast cancer. Among them, a siRNA targeting *MEK1* gene was designed. Their results showed a knockdown at the mRNA level of over 90% for *MEK1* and a knockdown at protein level of over 60% (Sahin et al., 2007). These results are better than the ones reported in the current work. However, it is important to notice that, besides the different siRNA sequence that was used, using different cell lines can also explain the discrepancies observed. In fact, a study performed on colon cancer cells (SW1116) the *MEK1* gene knockdown at the protein level was about 64% (Lu et al., 2007), which is more similar to our results.

Moreover, it is also visible a 52.1% knockdown of *ERK1* gene on Figure 17. Hence, the introduction of MEK1_siRNA on RKO cancer cells will decrease the *MEK1* gene expression and, consequently, will also reduce the *ERK1* gene expression to half. This gene is only activated by *MEK1* so it was expected a similar gene silencing decrease. As mention before, *ERK1* is directly involved in cell adhesion, which could possibly explain the decrease of cell proliferation and cell adhesion observed on the transfected cells.

Regarding the qRT-PCR results it is seen that the *MEK1* gene knockdown was not total. This could mean that only, at least, half of the cells were able to internalize the siRNA lipoplex and that on the remaining percentage of cells the *MEK1* gene is still expressed normally. There are other explanations for this event. First, it is possible that the siRNA lipoplex was internalized in a higher percentage of cells but the siRNA was not capable of escaping the lissome activity or it could be possible that the designed siRNA sequence was not specific enough for the mRNA targeted. The non-affected cells kept their function, retaining the continued activation of *ERK1* gene.

Eventually, as future work, the delivery system could be optimized by making the cells membrane more permeable or specific to the siRNA's complexes, for example by changing the siRNA encapsulation, thus enabling a higher siRNA internalization. One other possible improvement it could be the integration of a component in the siRNA encapsulation that may facilitate the endosomal escape.

# 4. Conclusion and Perspectives for Forthcoming work

The main goal of this project was the validation of a siRNA against *MEK1* for the treatment of colon cancer. To define which would be the cell line that should be used, several colon cancer cell lines were first cultured to assess the one with higher expression of the *MEK1* gene, through Western Blot. The cell line RKO was selected and the optimum siRNA concentration for an efficient transfection of these cells was found to be 30 nM.

Using this concentration of siRNA, a 52.5% knockdown of MEK1 at the protein level was determined by Western Blot. However, this is a semi-quantitative procedure that only provides a relative comparison between protein levels. To evaluate the transfection efficiency and also to quantify the gene knockdown, qRT-PCR was performed. The siRNA led to a 61.6% *MEK1* knockdown at the mRNA level. The effect of MEK1 knockdown on *ERK1*, a gene located downstream *MEK1*, was also evaluated through qRT-PCR. *ERK1* suffered a 52.1% knockdown. This gene is only activated by *MEK1* and it is directly involved on cell adhesion, which corroborates the decrease of cell adhesion and proliferation.

Similarly to the *ERK1* gene silencing study, the same could be done using the *WAVE-2* gene in future work. This gene is also located downstream *MEK1* but in this case, it is involved in cell migration, which is also an important factor regarding cancer therapy. In parallel, a migration assay could be performed to validate the possible effects on that gene.

Moreover, an improvement of the transfection efficiencies could be attempted through the use of better delivery agents. Several methodologies could be used such as, for instance, the combination of the siRNA with an aptamer to improve its recognition by the membrane receptors of the cells. Taking into account the endosomal-lysosome escape problem, some studies have been using chitosan nanocarriers to transfect breast cancer, which could also be a possibility for the current work.

A systematic evaluation of the MEK1 knockdown effects on cell cycle was herein studied through flow cytometry. The MEK1_siRNA transfection led to a cell cycle arrest on the G0-G1 phase, thus preventing the cells to get to S phase. Given that the DNA replication occurs on the S phase, these results strongly suggested that the cell proliferation may be affected by the *MEK1* silencing. As previously mentioned, these results are in accordance with reports from other researchers.

It is well known that the MAPK pathway has an important role on cell proliferation. Therefore, and thinking on the cell cycle results, the transfected cells viability was studied. The SRB results retrieved no significant differences between the MEK1_siRNA transfected cells and the controls. As the SRB experiment only quantifies the protein content, it was thought that although the number of cells remained the same perhaps they lost their proper function. Hence, to confirm that assumption a MTS assay was performed. The MTS assay measures the mitochondrial activity on metabolic active cells. The results

showed that the cells transfected with MEK1_siRNA exhibited a significant decrease of viability. This may indicate that cell arrest on G0-G1 corresponds to a cell cycle stop on the G0 checkpoint. At this point the cells stay in a quiescent state which means that the cells are alive but metabolic inactive. Increasing the experiment time could be a good way to have more reliable results and to better understand them.

In conclusion, the present study validated the ability of the designed siRNA sequence to target the *MEK1* gene and silencing its function, leading to a proliferation decrease on the colon cancer cell line used.

# 5. REFERENCES

**Ahmadzada, T., Reid, G., & McKenzie, D. R**. (2018). Fundamentals of siRNA and miRNA therapeutics and a review of targeted nanoparticle delivery systems in breast cancer. *Biophysical Reviews*, *10*(1), 69–86. https://doi.org/10.1007/s12551-017-0392-1

**Balko, J. M., Jones, B. R., Coakley, V. L., & Black, E. P.** (2009). MEK and EGFR inhibition demonstrate synergistic activity in EGFR-dependent NSCLC. *Cancer Biology & Therapy*, *8*(6), 522–530. https://doi.org/10.4161/cbt.8.6.7690

**Barbáchano, A., Larriba, M. J., Ferrer-Mayorga, G., González-Sancho, J. M., & Muñoz, A.** (2018). Vitamin D and Colon Cancer. In *Vitamin D* (pp. 837–862). Elsevier. https://doi.org/10.1016/B978-0-12-809963-6.00099-7

**Bennouna, J., Sastre, J., Arnold, D., Österlund, P., Greil, R., & Van Cutsem, E**. (2013). Continuation of bevacizumab after first progression in metastatic colorectal cancer (ML18147): a randomised phase 3 trial. *The Lancet Oncology*, *14*(1), 29–37. https://doi.org/10.1016/S1470-2045(12)70477-1

**Birmingham, A., Anderson, E., Sullivan, K., Reynolds, A., Boese, Q., & Leake, D.** (2007). A protocol for designing siRNAs with high functionality and specificity. *Nature Protocols*, *2*(9), 2068–2078. https://doi.org/10.1038/nprot.2007.278

**Bitko, V., Musiyenko, A., Shulyayeva, O., & Barik, S.** (2005). Inhibition of respiratory viruses by nasally administered siRNA. *Nature Medicine*, *11*(1), 50–55. https://doi.org/10.1038/nm1164

**Broeders, S., Huber, I., Grohmann, L., Berben, G., Taverniers, I., & Mazzara, M.** (2014). Guidelines for validation of qualitative real-time PCR methods. *Trends in Food Science & Technology*, *37*(2), 115–126. https://doi.org/10.1016/j.tifs.2014.03.008

**Buehler, E., Chen, Y.-C., & Martin, S.** (2012). C911: A Bench-Level Control for Sequence Specific siRNA Off-Target Effects. *PLoS ONE*, *7*(12), e51942. https://doi.org/10.1371/journal.pone.0051942

**Celalettin.** (2004). Understanding Colon Cancer. *Journal of the National Medical Association*, *96*(1), 120.

**De Luca, A., Maiello, M. R., D'Alessio, A., Pergameno, M., & Normanno, N.** (2012). The RAS/RAF/MEK/ERK and the PI3K/AKT signalling pathways: role in cancer pathogenesis and implications for therapeutic approaches. *Expert Opinion on Therapeutic Targets*, *16*(sup2), S17–S27. https://doi.org/10.1517/14728222.2011.639361

**Desjardins, P., & Conklin, D.** (2010). NanoDrop Microvolume Quantitation of Nucleic Acids. *Journal of Visualized Experiments*, (1). https://doi.org/10.3791/2565

**Druliner, B. R., Ruan, X., Sicotte, H., O'Brien, D., Liu, H., Kocher, J.-P. A., & Boardman, L.** (2018). Early genetic aberrations in patients with sporadic colorectal cancer. *Molecular Carcinogenesis*, *57*(1), 114–124. https://doi.org/10.1002/mc.22738

**Fang, J. Y., & Richardson, B. C.** (2005). The MAPK signalling pathways and colorectal cancer. *The Lancet Oncology*, *6*(5), 322–327. https://doi.org/10.1016/S1470-2045(05)70168-6

**Ferlay, J., Soerjomataram, I., Dikshit, R., Eser, S., Mathers, C., & Rebelo, M.** (2015). Cancer incidence and mortality worldwide: Sources, methods and major patterns in GLOBOCAN 2012. *International Journal of Cancer*, *136*(5), E359–E386. https://doi.org/10.1002/ijc.29210

**Ferreira, D., & Martins, I. M.** (2017). Artificial virus particles. In *Bioinspired Materials for Medical Applications* (pp. 427–450). Elsevier. https://doi.org/10.1016/B978-0-08-100741-9.00015-2

**Fire, A., Xu, S., Montgomery, M. K., Kostas, S. A., Driver, S. E., & Mello, C. C.** (1998). Potent and specific genetic interference by double-stranded RNA in Caenorhabditis elegans. *Nature*, *391*(6669), 806–811. https://doi.org/10.1038/35888

**Fleige, S., & Pfaffl, M. W.** (2006). RNA integrity and the effect on the real-time qRT-PCR performance. *Molecular Aspects of Medicine*, *27*(2–3), 126–139. https://doi.org/10.1016/j.mam.2005.12.003

**Fredericks, E., Dealtry, G., & Roux, S.** (2015). Molecular aspects of Colorectal Carcinogenesis : A Review, *3 (1): 105*, 1–8.

**Fujihara, K., Kotaki, M., & Ramakrishna, S.** (2005). Guided bone regeneration membrane made of polycaprolactone/calcium carbonate composite nano-fibers. *Biomaterials*, *26*(19), 4139–4147. https://doi.org/10.1016/j.biomaterials.2004.09.014

**Gajadhar, A. A., Reyes, J., & Lalonde, L. F.** (2013). Application of a qPCR Assay with Melting Curve Analysis for Detection and Differentiation of Protozoan Oocysts in Human Fecal Samples from Dominican Republic. *The American Journal of Tropical Medicine and Hygiene*, *89*(5), 892–898. https://doi.org/10.4269/ajtmh.13-0106

**Grinev, V. V.** (2012). Design and quality control of short interfering RNA. *Molecular Biology*, *46*(6), 739–754. https://doi.org/10.1134/S0026893312050056

**Han, C., Shin, A., Lee, J., Lee, J., Park, J. W., Oh, J. H., & Kim, J.** (2015). Dietary calcium intake and the risk of colorectal cancer: a case control study. *BMC Cancer*, *15*(1), 966. https://doi.org/10.1186/s12885-015-1963-9

**Hardy, R. G.** (2000). ABC of colorectal cancer: Molecular basis for risk factors. *BMJ*, *321*(7265), 886–889. https://doi.org/10.1136/bmj.321.7265.886

**Heinemann, V., von Weikersthal, L. F., Decker, T., Kiani, A., Vehling-Kaiser, U., & Al-Batran, S.-E.** (2014). FOLFIRI plus cetuximab versus FOLFIRI plus bevacizumab as first-line treatment for patients with metastatic colorectal cancer (FIRE-3): a randomised, open-label, phase 3 trial. *The Lancet Oncology*, *15*(10), 1065–1075. https://doi.org/10.1016/S1470-2045(14)70330-4

**Hofmann, S. L., Russell, D. W., Goldstein, J. L., & Brown, M. S.** (1987). mRNA for low density lipoprotein receptor in brain and spinal cord of immature and mature rabbits. *Proceedings of the National Academy of Sciences*, *84*(17), 6312–6316. https://doi.org/10.1073/pnas.84.17.6312

**Jackson, A. L., & Linsley, P. S.** (2010). Recognizing and avoiding siRNA off-target effects for target identification and therapeutic application. *Nature Reviews Drug Discovery*, *9*(1), 57–67. https://doi.org/10.1038/nrd3010

**Jain, S., Pathak, K., & Vaidya, A.** (2018). Molecular therapy using siRNA: Recent trends and advances of multi target inhibition of cancer growth. *International Journal of Biological Macromolecules*, *116*, 880–892. https://doi.org/10.1016/j.ijbiomac.2018.05.077

**Karim, M., Tha, K., Othman, I., Borhan Uddin, M., & Chowdhury, E.** (2018). Therapeutic Potency of Nanoformulations of siRNAs and shRNAs in Animal Models of Cancers. *Pharmaceutics*, *10*(2), 65. https://doi.org/10.3390/pharmaceutics10020065

**Kennelly, R. P., Gryfe, R., & Winter, D. C.** (2017). Familial colorectal cancer: Patient assessment, surveillance and surgical management. *European Journal of Surgical Oncology (EJSO)*, *43*(2), 294–302. https://doi.org/10.1016/j.ejso.2016.07.008

**Ki, K. H., Park, D. Y., Lee, S. H., Kim, N. Y., Choi, B. M., & Noh, G. J.** (2010). The optimal concentration of siRNA for gene silencing in primary cultured astrocytes and microglial cells of rats. *Korean Journal of Anesthesiology*, *59*(6), 403. https://doi.org/10.4097/kjae.2010.59.6.403

**Kim, T. K., & Eberwine, J. H.** (2010). Mammalian cell transfection: the present and the future. *Analytical and Bioanalytical Chemistry*, *397*(8), 3173–3178. https://doi.org/10.1007/s00216-010-3821-6

**Kurien, B. T., & Scofield, R. H.** (2006, April). Western blotting. *Methods*. https://doi.org/10.1016/j.ymeth.2005.11.007

**Laporte, G. A., Leguisamo, N. M., Kalil, A. N., & Saffi, J.** (2018). Clinical importance of DNA repair in sporadic colorectal cancer. *Critical Reviews in Oncology/Hematology*, *126*, 168–185. https://doi.org/10.1016/j.critrevonc.2018.03.017

**Lu, R., Wang, X., Chen, Z.-F., Sun, D.-F., Tian, X.-Q., & Fang, J.-Y.** (2007). Inhibition of the Extracellular Signal-regulated Kinase/Mitogen-activated Protein Kinase Pathway Decreases DNA Methylation in Colon Cancer Cells. *Journal of Biological Chemistry*, *282*(16), 12249–12259. https://doi.org/10.1074/jbc.M608525200

**Majzoub, R. N., Ewert, K. K., & Safinya, C. R.** (2016). Cationic liposome–nucleic acid nanoparticle assemblies with applications in gene delivery and gene silencing. *Philosophical Transactions of the Royal Society A: Mathematical, Physical and Engineering Sciences*, *374*(2072), 20150129.

https://doi.org/10.1098/rsta.2015.0129

**McCubrey, J. A., Steelman, L. S., Chappell, W. H., Abrams, S. L., Wong, E. W. T., & Chang, F.** (2007). Roles of the Raf/MEK/ERK pathway in cell growth, malignant transformation and drug resistance. *Biochimica et Biophysica Acta (BBA) - Molecular Cell Research*, *1773*(8), 1263–1284. https://doi.org/10.1016/j.bbamcr.2006.10.001

**McNaughton, B. R., Cronican, J. J., Thompson, D. B., & Liu, D. R.** (2009). Mammalian cell penetration, siRNA transfection, and DNA transfection by supercharged proteins. *Proceedings of the National Academy of Sciences*, *106*(15), 6111–6116. https://doi.org/10.1073/pnas.0807883106

**Menges, C. W., & McCance, D. J.** (2008). Constitutive activation of the Raf–MAPK pathway causes negative feedback inhibition of Ras–PI3K–AKT and cellular arrest through the EphA2 receptor. *Oncogene*, *27*(20), 2934–2940. https://doi.org/10.1038/sj.onc.1210957

**Mocellin, S., & Provenzano, M.** (2004). No Title. *Journal of Translational Medicine*, *2*(1), 39. https://doi.org/10.1186/1479-5876-2-39

**Mundade, R., Imperiale, T. F., Prabhu, L., Loehrer, P. J., & Lu, T.** (2014). Genetic pathways, prevention, and treatment of sporadic colorectal cancer. *Oncoscience*, *1*, 400. https://doi.org/10.18632/oncoscience.59

**Napoli, C.** (1990). Introduction of a Chimeric Chalcone Synthase Gene into Petunia Results in Reversible Co-Suppression of Homologous Genes in trans. *THE PLANT CELL ONLINE*, *2*(4), 279–289. https://doi.org/10.1105/tpc.2.4.279

**Oh, Y.-T., Deng, J., Yue, P., Owonikoko, T. K., Khuri, F. R., & Sun, S.-Y.** (2016). Inhibition of B-Raf/MEK/ERK signaling suppresses DR5 expression and impairs response of cancer cells to DR5-mediated apoptosis and T cell-induced killing. *Oncogene*, *35*(4), 459–467. https://doi.org/10.1038/onc.2015.97

**Pan, P., Yu, J., & Wang, L.-S.** (2018). Colon Cancer. *Surgical Oncology Clinics of North America*, *27*(2), 243–267. https://doi.org/10.1016/j.soc.2017.11.002

**Pietrzyk, Ł.** (2017). Food properties and dietary habits in colorectal cancer prevention and development. *International Journal of Food Properties*, *20*(10), 2323–2343. https://doi.org/10.1080/10942912.2016.1236813

**Rana, T. M.** (2007). Illuminating the silence: understanding the structure and function of small RNAs. *Nature Reviews Molecular Cell Biology*, *8*(1), 23–36. https://doi.org/10.1038/nrm2085

**Reynolds, A., Leake, D., Boese, Q., Scaringe, S., Marshall, W. S., & Khvorova, A.** (2004). Rational siRNA design for RNA interference. *Nature Biotechnology*, *22*(3), 326–330.

https://doi.org/10.1038/nbt936

**Rezvani Amin, Z., Rahimizadeh, M., Eshghi, H., Dehshahri, A., & Ramezani, M.** (2013). The effect of cationic charge density change on transfection efficiency of polyethylenimine. *Iranian Journal of Basic Medical Sciences*, *16*(2), 150–6. Retrieved from http://www.ncbi.nlm.nih.gov/pubmed/24298383

**Sahin, O., Lobke, C., Korf, U., Appelhans, H., Sultmann, H., & Poustka, A.** (2007). Combinatorial RNAi for quantitative protein network analysis. *Proceedings of the National Academy of Sciences*, *104*(16), 6579–6584. https://doi.org/10.1073/pnas.0606827104

**Schafer, K. A.** (1998). The Cell Cycle: A Review. *Veterinary Pathology*, *35*(6), 461–478. https://doi.org/10.1177/030098589803500601

**Schmitz, J. C., & Chu, E.** (2011). Effect of small interfering RNA 3'-end overhangs on chemosensitivity to thymidylate synthase inhibitors. *Silence*, *2*(1), 1. https://doi.org/10.1186/1758-907X-2-1

**Sebolt-Leopold, J. S., Dudley, D. T., Herrera, R., Becelaere, K. Van, Wiland, A., & Gowan, R. C.** (1999). Blockade of the MAP kinase pathway suppresses growth of colon tumors in vivo. *Nature Medicine*, *5*(7), 810–816. https://doi.org/10.1038/10533

**Seidel, D. V., Azcárate-Peril, M. A., Chapkin, R. S., & Turner, N. D.** (2017). Shaping functional gut microbiota using dietary bioactives to reduce colon cancer risk. *Seminars in Cancer Biology*, *46*, 191–204. https://doi.org/10.1016/j.semcancer.2017.06.009

**Siegel, R. L., Miller, K. D., & Jemal, A.** (2017). Cancer statistics, 2017. *CA: A Cancer Journal for Clinicians*, *67*(1), 7–30. https://doi.org/10.3322/caac.21387

**Tariq, K., & Ghias, K.** (2016). Colorectal cancer carcinogenesis: a review of mechanisms. *Cancer Biology & Medicine*, *13*(1), 120–35. https://doi.org/10.28092/j.issn.2095-3941.2015.0103

**Urosevic, J., Nebreda, A. R., & Gomis, R. R.** (2014). MAPK signaling control of colon cancer metastasis. *Cell Cycle*, *13*(17), 2641–2642. https://doi.org/10.4161/15384101.2014.946374

**Valentino, J. D., Elliott, V. A., Zaytseva, Y. Y., Rychahou, P. G., Mustain, W. C., & Wang, C.** (2012). Novel small interfering RNA cotargeting strategy as treatment for colorectal cancer. *Surgery*, *152*(2), 277–285. https://doi.org/10.1016/j.surg.2012.05.006

**Veenstra, C., & Krauss, J.** (2018). Emerging Systemic Therapies for Colorectal Cancer. *Clinics in Colon and Rectal Surgery*, *31*(3), 179–191. https://doi.org/10.1055/s-0037-1602238

**Villanueva, J., Vultur, A., Lee, J. T., Somasundaram, R., Fukunaga-Kalabis, M., & Cipolla, A. K.** (2010). Acquired Resistance to BRAF Inhibitors Mediated by a RAF Kinase Switch in Melanoma Can Be Overcome by Cotargeting MEK and IGF-1R/PI3K. *Cancer Cell*, *18*(6), 683–695.

https://doi.org/10.1016/j.ccr.2010.11.023

**Whitehead, K. A., Langer, R., & Anderson, D. G.** (2009). Knocking down barriers: advances in siRNA delivery. *Nature Reviews Drug Discovery*, *8*(2), 129–138. https://doi.org/10.1038/nrd2742

**WHO** | Estimates for 2000–2015. (2017). *WHO*. Retrieved from http://www.who.int/healthinfo/global_burden_disease/estimates/en/index1.html

**Wolpin, B. M., & Mayer, R. J.** (2008). Systemic Treatment of Colorectal Cancer. *Gastroenterology*, *134*(5), 1296–1310.e1. https://doi.org/10.1053/j.gastro.2008.02.098

**You, X., Kang, Y., Hollett, G., Chen, X., Zhao, W., Gu, Z., & Wu, J.** (2016). Polymeric nanoparticles for colon cancer therapy: overview and perspectives. *Journal of Materials Chemistry B*, *4*(48), 7779–7792. https://doi.org/10.1039/C6TB01925K

**Zhang, W., & Liu, H. T.** (2002). MAPK signal pathways in the regulation of cell proliferation in mammalian cells. *Cell Research*, *12*(1), 9–18. https://doi.org/10.1038/sj.cr.7290105

**Zhang, X.-Q., Zhang, H.-M., Sun, X.-E., Yuan, Z.-J., & Feng, Y.-G.** (2015). Inhibitory effects and mechanism of 5-fluorouracil combined with celecoxib on human gastric cancer xenografts in nude mice. *Experimental and Therapeutic Medicine*, *9*(1), 105–111. https://doi.org/10.3892/etm.2014.2077

**Zuckerman, J. E., & Davis, M. E.** (2015). Clinical experiences with systemically administered siRNA-based therapeutics in cancer. *Nature Reviews Drug Discovery*, *14*(12), 843–856. https://doi.org/10.1038/nrd4685

# 6. SUPPLEMENTARY DATA

## Supplementary data A – BSA calibration curve

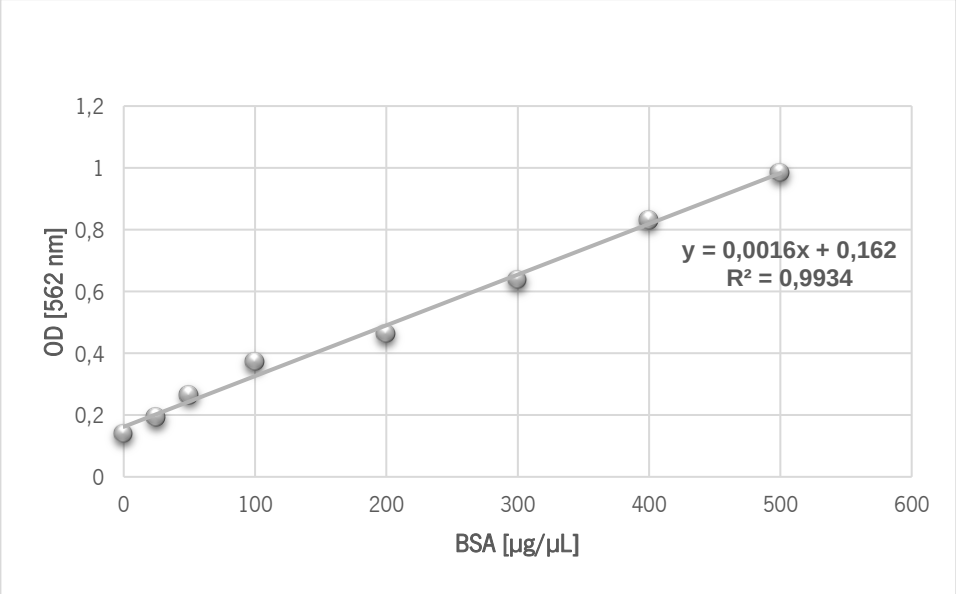


**Figure A. 1** – Calibration curve of BSA protein standards

## Supplementary data B – qRT-PCR calibration curves

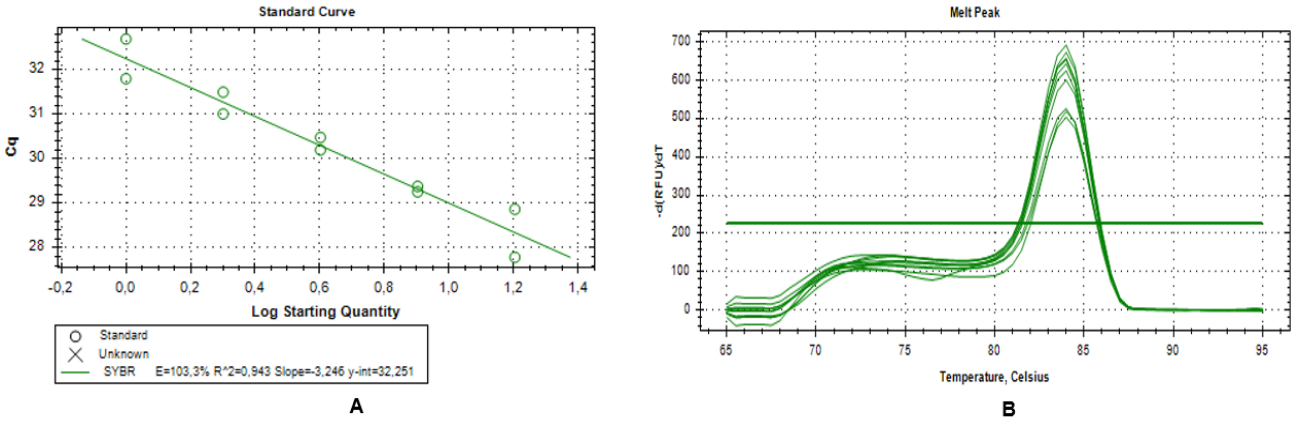


**Figure B. 1 –** Standard (A) and Melt Curve (B) generated from the total RNA extracted from RKO cells using specific primers for the housekeeping gene GADPH.

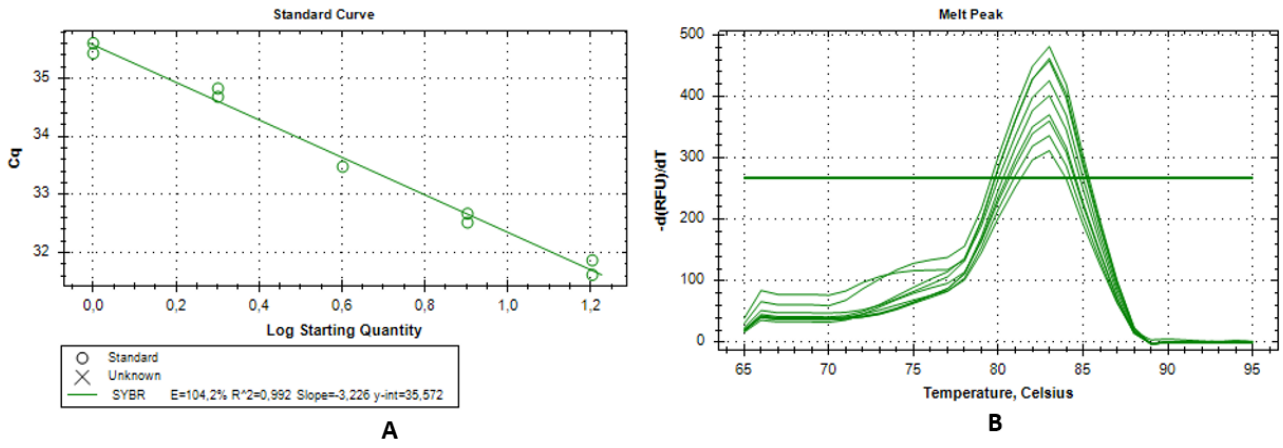


**Figure B. 2** – Standard (A) and Melt Curve (B) generated from the total RNA extracted from RKO cells using specific primers for the gene MEK1.

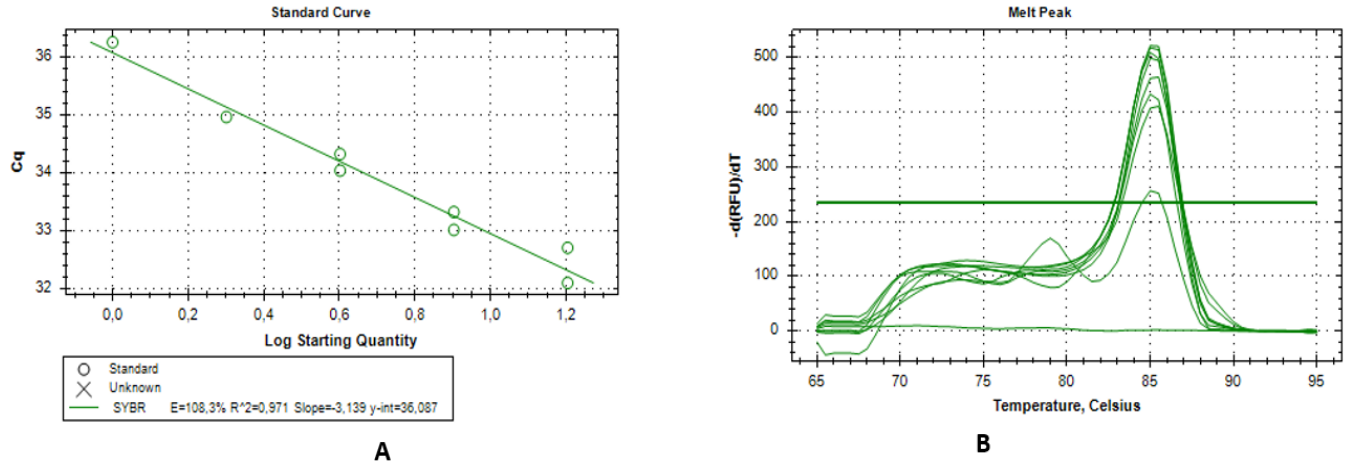


**Figure B. 3 -** Standard (A) and Melt Curve (B) generated from the total RNA extracted from RKO cells using specific primers for the gene ERK1.